

# Revisiting semi-leptonic decays of $\Lambda_{b(c)}$ supported by baryon spectroscopy

Yu-Shuai Li<sup>1,2,\*</sup>, Xiang Liu<sup>1,2,3,†</sup> and Fu-Sheng Yu<sup>3,4,5,‡</sup>

<sup>1</sup>*School of Physical Science and Technology, Lanzhou University, Lanzhou 730000, China*

<sup>2</sup>*Research Center for Hadron and CSR Physics, Lanzhou University and Institute of Modern Physics of CAS, Lanzhou 730000, China*

<sup>3</sup>*Lanzhou Center for Theoretical Physics, Key Laboratory of Theoretical Physics of Gansu Province, and Frontiers Science Center for Rare Isotopes, Lanzhou University, Lanzhou 730000, China*

<sup>4</sup>*School of Nuclear Science and Technology, Lanzhou University, Lanzhou 730000, China*

<sup>5</sup>*Center for High Energy Physics, Peking University, Beijing 100871, China*

The semi-leptonic decays of  $\Lambda_b \rightarrow \Lambda_c^{(*)} \ell \nu_\ell$  and  $\Lambda_c \rightarrow \Lambda^{(*)} \ell \nu_\ell$  are studied in the light-front quark model in this work. Instead of the quark-diquark approximation, we use the three-body wave functions obtained by the involving baryon spectroscopy. The ground states ( $1/2^+$ ), the  $\lambda$ -mode orbital excited states ( $1/2^-$ ) and the first radial excited states ( $1/2^+$ ) of  $\Lambda_c^{(*)}$  are considered. The discussions are given for the form factors, partial widths, branching fractions, leptonic forward-backward asymmetries, hadron polarizations, lepton polarizations, and the lepton flavor universalities. Our results are useful for the inputs of heavy baryon decays and understanding the baryon structures, and helpful for the experimental measurements.

## I. INTRODUCTION

In recent years, a lot of progresses have been made in the weak decays of heavy-flavor baryons, such as the observation of the double-charm baryon  $\Xi_{cc}^{++}$  [1, 2], the first measurements of the absolute branching fractions of  $\Lambda_c^+$  and  $\Xi_c^{+0}$  decays [3–8], and the evidence of  $CP$  violation in  $\Lambda_b^0 \rightarrow p\pi^+\pi^-\pi^-$  [9]. The semi-leptonic decays play an important role in the understanding of the dynamics of beauty and charm baryon decays. The simpler dynamics of semi-leptonic decays compared to the non-leptonic ones, can help to search for the new physics beyond the Standard Model and study the structures of excited states of baryons.

The lepton flavor universality violation (LFUV) was tested in the recent years by the ratio of  $R(D^{(*)}) = \mathcal{B}(B \rightarrow D^{(*)}\tau\nu_\tau)/\mathcal{B}(B \rightarrow D^{(*)}e(\mu)\nu_{e(\mu)})$ . The experimental measurements deviate from the Standard Model (SM) predictions by  $3.1\sigma$  [10], indicating a hint for new physics. It was pointed out that the  $\Lambda_b \rightarrow \Lambda_c \ell \nu$  decays provide a theoretical cleaner place to test the LFUV [11, 12]. Up to the order of  $\mathcal{O}(\Lambda_{\text{QCD}}^2/m_c^2)$  in the heavy quark effective theory, there are only three Isgur-Wise functions in the  $\Lambda_b \rightarrow \Lambda_c$  transitions, compared to the 10 parameters in  $B \rightarrow D^{(*)}$  transitions. Due to the large data collected by LHCb in the near future, some excited states involved processes of  $\Lambda_b \rightarrow \Lambda_c^* \ell \nu_\ell$  can also be measured [13]. Thus, it deserves to systematically study the  $\Lambda_b \rightarrow \Lambda_c^{(*)} \ell \nu_\ell$  decays in the same theoretical framework.

The comparison between the semi-leptonic exclusive decay of  $\Lambda_c^+ \rightarrow \Lambda e^+ \nu_e$  and the inclusive  $\Lambda_c^+ \rightarrow e^+ X$  decay provides an interesting result. The BESIII measurements show that the branching fraction of the exclusive process of  $\mathcal{B}(\Lambda_c^+ \rightarrow \Lambda e^+ \nu_e) = (3.63 \pm 0.43)\%$  [4], dominates the inclusive decay of  $\mathcal{B}(\Lambda_c^+ \rightarrow e^+ X) = (3.95 \pm 0.35)\%$  [7], with a fraction of  $(91.9 \pm 13.6)\%$ . It implies a little room for other semi-leptonic processes involving excited final states. This

phenomenon is quite different from the charmed meson decays. For example,  $\mathcal{B}(D^+ \rightarrow \bar{K}^0 e^+ \nu_e) = (8.73 \pm 0.10)\%$  is much smaller than  $\mathcal{B}(D^+ \rightarrow e^+ X) = (16.07 \pm 0.30)\%$  [14]. Therefore, it is necessary to explore the excited-state involving processes of  $\Lambda_c^+ \rightarrow \Lambda^{(*)} e^+ \nu_e$ , to solve this problem.

The key issue in the theoretical study of semi-leptonic decays is to calculate the weak transition form factors. They are also the important inputs in the non-leptonic decays, such as in the prediction of the discovery channels of the doubly charmed baryons [15–18]. The current researching status on the form factors is reviewed in the next section. The main difficulty in the calculations is from the three-body problem in the baryons. A lot of theoretical works are based on the approximation of the quark-diquark scheme [19–23].

In this work, we calculate the form factors of  $\Lambda_b \rightarrow \Lambda_c^{(*)} (1/2^\pm)$  and  $\Lambda_c \rightarrow \Lambda^{(*)} (1/2^\pm)$  transitions in the light-front quark model with a triquark picture. There are some important improvements. Firstly, the triquark picture is more close to the conventional baryons' structures, compared to the diquark approximation. Secondly, the baryons' wave functions are obtained by the Gaussian Expansion Method (GEM), avoiding the effective parameters  $\beta$ 's which are the major uncertainties in the previous works [16, 19–21, 24, 25]. Finally, the parameters in the wave functions are fixed by the baryon spectra, since a series of baryons are involved in this work.

The organization of this paper is as follows. In Sec. II, the current research status on the theoretical calculations of form factors are given. In Sec. III, the formalisms for the form factors of the related processes are derived in the framework of light-front quark model. The formulas of Godfrey-Isgure (GI) model and GEM, which used to obtain the spatial wave functions of baryons, are illustrated. In Sec. IV, we give our numerical results, either the spatial wave functions for involved baryons, or the numerical results of form factors. Besides, the relevant semi-leptonic differential decay rates and the branching fractions are also obtained by using these form factors. We also made a comparison with other theoretical predictions and experimental data. The conclusion and discussion are given in the last section.

\*Electronic address: liysh20@lzu.edu.cn

†Electronic address: xiangliu@lzu.edu.cn

‡Electronic address: yufsh@lzu.edu.cn

## II. THE PRESENT RESEARCH STATUS

The semi-leptonic decays of  $\Lambda_Q$  had been widely studied with various approaches, which include flavor symmetry, various quark models, light-front approach, QCD sum rules (QCDSR), Light-cone sum rules (LCSR), Lattice QCD (LQCD) and so on. In this section, we briefly introduce the present status of the semi-leptonic decays of  $\Lambda_Q$ .

In the early 1980s, the evidence of  $\Lambda_c^+$  semi-leptonic decay [26, 27] was found. However, the precisions on the branching ratios were very low in the experiments [28–30]. The recent progress on this issue was made by the BESIII Collaboration [4, 6], where the first measurement of the absolute branching ratio for  $\Lambda_c^+ \rightarrow \Lambda \ell^+ \nu_\ell$  was given

$$\begin{aligned} \mathcal{B}(\Lambda_c^+ \rightarrow \Lambda e^+ \nu_e) &= (3.63 \pm 0.38 \pm 0.20)\%, \\ \mathcal{B}(\Lambda_c^+ \rightarrow \Lambda \mu^+ \nu_\mu) &= (3.49 \pm 0.46 \pm 0.27)\%. \end{aligned}$$

Obviously, the newly measurement can be applied to test the different theoretical approaches describing the  $\Lambda_c^+$  semi-leptonic decays.

In 1989, Marcial *et al.* [31] predicted the widths and branching fractions of  $\Lambda_c^+ \rightarrow \Lambda e^+ \nu_e$  by using both nonrelativistic quark model and MIT bag model. Here, the predicted branching ratio of  $\mathcal{B}(\Lambda_c^+ \rightarrow \Lambda e^+ \nu_e)$  is 1.4 ~ 4.2 %. Later, Hussain and Korner [32] studied the same topic with a relativistic spectator quark model, where the interaction between the spectator quark and the acting quark is ignored. This treatment was widely used in the study of heavy to heavy transitions, and was expanded to  $c \rightarrow s$  sector by them. The estimated branching fraction is 4.45% [32]. Efimov *et al.* also focused on  $\Lambda_c^+ \rightarrow \Lambda e^+ \nu_e$  decay at the same time. By the quark confinement model, they predicted  $\mathcal{B}(\Lambda_c^+ \rightarrow \Lambda e^+ \nu_e) = 5.72\%$  [33]. Cheng and Tseng [34] applied the nonrelativistic quark model and considered the flavor suppression factor, and obtained  $\mathcal{B}(\Lambda_c^+ \rightarrow \Lambda e^+ \nu_e) = 1.44\%$ . In fact, QCDSR is also an effective approach to study the semi-leptonic decay of  $\Lambda_c$ . For example, Carvalho *et al.* estimated  $\mathcal{B}(\Lambda_c^+ \rightarrow \Lambda e^+ \nu_e) = (2.69 \pm 0.37)\%$  [35]. By including the higher twist contributions in the light-cone sum rule calculation, Liu *et al.* [36] calculated  $\mathcal{B}(\Lambda_c^+ \rightarrow \Lambda l^+ \nu_l)$ , which is 3.0% or 2.0% if adopting Chernyak-Zhitnitsky-type or Ioffe-type interpolating current, respectively. In addition, Zhao *et al.* [37] also presented the involved form factors and decay rates in QCDSR, where the results are consistent with the experimental data within errors. Pervin *et al.* [38] performed the calculation in the framework of consistent quark model with both nonrelativistic and semirelativistic Hamiltonians. The obtained decay rate from semirelativistic Hamiltonian can well describe the experimental data, while the one from nonrelativistic Hamiltonian shows apparent divergence [38]. Migura *et al.* used a relativistically covariant constituent quark model with Bethe-Salpeter equation and found  $\mathcal{B}(\Lambda_c^+ \rightarrow \Lambda e^+ \nu_e) = 3.19\%$  and  $\mathcal{B}(\Lambda_c^+ \rightarrow \Lambda \mu^+ \nu_\mu) = 2.97\%$  [39].

After measuring the absolute branching fractions of  $\mathcal{B}(\Lambda_c^+ \rightarrow \Lambda \ell^+ \nu_\ell)$  by BESIII [4, 6], Faustov and Galkin [40] investigated the semi-leptonic decays of  $\Lambda_c$  within relativistic quark model (RQM) based on quasipotential approach. By

taking into account the relativistic effects, their estimations for  $\mathcal{B}(\Lambda_c^+ \rightarrow \Lambda e^+ \nu_e)$  and  $\mathcal{B}(\Lambda_c^+ \rightarrow \Lambda \mu^+ \nu_\mu)$  are 3.25% and 3.14%, respectively, which are well comparable with the current measurements. Besides, Gutsche *et al.* [41] applied the covariant confined quark model (CCQM). Apart from the decay rates, they also presented some detailed results for other physical observables, which are also important to the study of semi-leptonic decay. The light-front approach was also widely used to analyze the semi-leptonic decays of  $\Lambda_c$ . Zhao [23] studied the  $\Lambda_c^+ \rightarrow \Lambda e^+ \nu_e$  process in the light-front approach by treating the spectator quarks as a diquark system and used an effective parameter to simulate the baryon wave function. With this approximation, he obtained  $\mathcal{B}(\Lambda_c^+ \rightarrow \Lambda e^+ \nu_e) = 1.63\%$ , which is smaller than the BESIII data. On the contrary, without considering diquark approximation, Geng *et al.* [25] estimated  $\mathcal{B}(\Lambda_c^+ \rightarrow \Lambda e^+ \nu_e) = (3.36 \pm 0.87)\%$  and  $\mathcal{B}(\Lambda_c^+ \rightarrow \Lambda \mu^+ \nu_\mu) = (3.21 \pm 0.85)\%$ , which can well reproduce the BESIII data.

In the following, we continue to introduce the research status of the semi-leptonic decays of  $\Lambda_b$ . Firstly, we should show the current experimental data in Particle Data Group (PDG) [14]

$$\begin{aligned} \mathcal{B}(\Lambda_b \rightarrow \Lambda_c^+ \ell^- \nu_\ell) &= (6.4_{-1.3}^{+1.4})\%, \\ \mathcal{B}(\Lambda_b \rightarrow \Lambda_c(2595)^+ \ell^- \nu_\ell) &= (0.79_{-0.35}^{+0.40})\% \end{aligned} \quad (1)$$

with  $\ell^- = e^-$  or  $\mu^-$ . Obviously, there still need some improvement in these measurements.

The  $\Lambda_b \rightarrow \Lambda_c^+ \ell^- \nu_\ell$  semi-leptonic decays have been studied for a long time [35, 42–50]. Different from the  $\Lambda_c^+$  semi-leptonic decays, the  $\tau^-$ -mode of the  $\Lambda_b \rightarrow \Lambda_c^+ \ell^- \nu_\ell$  semi-leptonic decay is allowed kinematically. Similar to the discussion of the  $B \rightarrow D^{(*)}$  semi-leptonic decays [51, 52], investigating the ratio  $R(\Lambda_c) = \mathcal{B}(\Lambda_b \rightarrow \Lambda_c^+ \ell^- \nu_\ell) / \mathcal{B}(\Lambda_b \rightarrow \Lambda_c^+ \tau^- \nu_\tau)$  with  $\ell^- = e^-$  or  $\mu^-$  is also an interesting research topic. Thus, in this work, we will focus on this issue. There were some theoretical investigations of the  $\Lambda_b$  semi-leptonic decays. Ke *et al.* [20, 21, 24] calculated the branching fractions in standard and covariant light-front quark models within diquark picture. Their results show that the quark-diquark picture works well for heavy baryons. Besides, they also reinvestigated the same topic by the same approach without introducing diquark approximation. A RQM [53, 54] with quark-diquark approximation was used by Ebert, Faustov and Galkin. The calculated branching fractions is consistent with the experimental data. And, other physical observables were also given. Gutsche *et al.* [55, 56] calculated the  $\Lambda_b \rightarrow \Lambda_c^+ \ell^- \nu_\ell$  ( $\ell^- = e^-, \mu^-, \tau^-$ ) observables by using the covariant confined quark model. Ranmani *et al.* [57] calculated them in a potential model with a modified QCD Cornell interaction. Thakkar [58] studied the semi-leptonic decays by using the hypercentral constituent quark model, where the six-dimensional hypercentral Schrödinger equation was solved for extracting the wave functions of heavy baryons. Of course, the QCDSR was also applied to the study of the  $\Lambda_b$  semi-leptonic decays [59–62].

Until now, theorist has paid more attentions to the semi-leptonic decays of  $\Lambda_Q$  to a ground state of  $\Lambda$  or  $\Lambda_c$ . Since 2005, the semi-leptonic decays of  $\Lambda_Q$  to an excited state of  $\Lambda$  or  $\Lambda_c$  have been studied. Pervin *et al.* [38] studied

the semi-leptonic decays of  $\Lambda_Q$  to  $J^P = \frac{1}{2}^\pm, \frac{3}{2}^-$  final states in a constituent quark model with both nonrelativistic and semirelativistic Hamiltonians. Gussain and Roberts [63] studied the semileptonic decays of  $\Lambda_c^+$  to excited  $\Lambda$  states with a nonrelativistic quark model. Gutsche *et al.* [56] analyzed  $\Lambda_b \rightarrow \Lambda_c \left(\frac{1}{2}^\pm, \frac{3}{2}^-\right) \ell^- \nu_\ell$  with CCQM. Nieves *et al.* [64] studied the  $\Lambda_b \rightarrow \Lambda_c(2595, 2625) \ell^- \nu_\ell$  with heavy quark spin symmetry. Bečirević *et al.* [65] studied  $\Lambda_b \rightarrow \Lambda_c \left(\frac{1}{2}^\pm\right) \ell^- \nu_\ell$  by using the Bakamjian-Thomas approach with a spectroscopic model. Recently, the BESIII Collaboration [66] released a white paper of future plan, where measuring  $\Lambda_c \rightarrow \Lambda^* \ell^+ \nu_\ell$  was mentioned. For enlarging our knowledge on the semi-leptonic decays of  $\Lambda_Q$  to excited  $\Lambda$  or  $\Lambda_c$  state, joint effort from experimentalist and theorist is needed.

In fact, the Lattice QCD (LQCD) [67–71] is an effective approach to study the  $\Lambda_Q$  semi-leptonic decays. Meinal *et al.* [69, 71] calculated the form factors and decay rates of  $\Lambda_b \rightarrow \Lambda_c \ell^- \nu_\ell$  and  $\Lambda_c \rightarrow \Lambda \ell^+ \nu_\ell$  processes with all possible leptonic channels. Very recently, they presented the first Lattice QCD calculation of the form factors describing the  $\Lambda_b \rightarrow \Lambda_c \left(\frac{1}{2}^-, \frac{3}{2}^-\right) \ell^- \nu_\ell$  decays [70]. We are looking forward more progresses on the  $\Lambda_Q$  semi-leptonic decays by LQCD, which may provide valuable information to theoretical studies.

The numerical results from literatures are summarized in the table in Sec. V, with a comparison to our predictions.

### III. SEMI-LEPTONIC DECAYS OF $\Lambda_Q$

#### A. The form factors relevant to semi-leptonic decays of $\Lambda_Q$

In this subsection, we briefly present how to calculate the form factors involved in these semi-leptonic decays of  $\Lambda_b$  and  $\Lambda_c$ . For illustration, we take  $\Lambda_b \rightarrow \Lambda_c^*(1/2^\pm)$  as an example, where  $\Lambda_c(1/2^+)$  and  $\Lambda_c(1/2^-)$  denote  $\Lambda_c(2286)$  and  $\Lambda_c(2595)$ , respectively. In addition, we use subscript \* to mark the radial excitation.

The Hamiltonian depicting corresponding semi-leptonic decays is written as

$$\mathcal{H}_{eff} = \frac{G_F}{\sqrt{2}} V_{cb} \bar{\ell} \gamma_\mu (1 - \gamma_5) \nu_\ell \bar{c} \gamma^\mu (1 - \gamma_5) b, \quad (2)$$

where  $G_F$  is the Fermi constant and  $V_{cb}$  is the CKM matrix element. In Fig. 1, the Feynman diagram for the weak transition is given.

Given that the quarks are confined in hadron, the weak transition matrix element cannot be calculated by QCD since these weak transitions are involved in low-energy aspects of QCD. Generally, the matrix elements of hadron section  $\langle \Lambda_c^*(1/2^\pm) | \bar{c} \gamma^\mu (1 - \gamma_5) b | \Lambda_b(1/2^+) \rangle$  can be parameterized in terms of several dimensionless form factors as

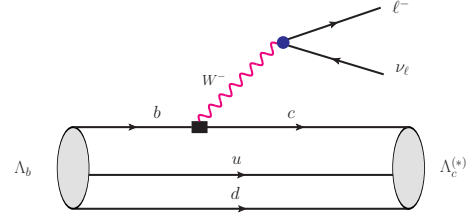


FIG. 1: The diagram for depicting the  $\Lambda_b \rightarrow \Lambda_c^* \ell^- \nu_\ell$  decays in tree level.

$$\begin{aligned} & \langle \Lambda_c^*(1/2^+)(P', J'_z) | \bar{c} \gamma^\mu (1 - \gamma_5) b | \Lambda_b(P, J_z) \rangle \\ &= \bar{u}(P', J'_z) \left[ f_1^V(q^2) \gamma^\mu + i \frac{f_2^V(q^2)}{M} \sigma^{\mu\nu} q_\nu + \frac{f_3^V(q^2)}{M} q^\mu \right. \\ & \quad \left. - \left( g_1^A(q^2) \gamma^\mu + i \frac{g_2^A(q^2)}{M} \sigma^{\mu\nu} q_\nu + \frac{g_3^A(q^2)}{M} q^\mu \right) \gamma_5 \right] u(P, J_z), \end{aligned} \quad (3)$$

$$\begin{aligned} & \langle \Lambda_c(1/2^-)(P', J'_z) | \bar{c} \gamma^\mu (1 - \gamma_5) b | \Lambda_b(P, J_z) \rangle \\ &= \bar{u}(P', J'_z) \left[ \left( g_1^V(q^2) \gamma^\mu + i \frac{g_2^V(q^2)}{M} \sigma^{\mu\nu} q_\nu + \frac{g_3^V(q^2)}{M} q^\mu \right) \gamma_5 \right. \\ & \quad \left. - \left( f_1^A(q^2) \gamma^\mu + i \frac{f_2^A(q^2)}{M} \sigma^{\mu\nu} q_\nu + \frac{f_3^A(q^2)}{M} q^\mu \right) \right] u(P, J_z), \end{aligned} \quad (4)$$

for  $1/2^+ \rightarrow 1/2^+$  and  $1/2^+ \rightarrow 1/2^-$  transitions, respectively. Here,  $M(P)$ ,  $M'(P')$  denote the masses (four momentums) of the initial and final hadrons respectively, and  $q = P - P'$ .

Following the standard procedure, the angular distribution for the decay  $\Lambda_b \rightarrow \Lambda_c^* W^- (\rightarrow \ell^- \bar{\nu}_\ell)$  reads as

$$\begin{aligned} \frac{d\Gamma}{dq^2 d \cos \theta_l} &= \frac{G_F^2}{(2\pi)^3} |V_{cb}|^2 \frac{\sqrt{\lambda(M^2, M'^2, q^2)} (q^2 - m_l^2)^2}{128 M^3 q^2} \\ & \quad \times \left[ A_1 + \frac{m_l^2}{q^2} A_2 \right], \end{aligned} \quad (5)$$

where  $\lambda(x, y, z) = x^2 + y^2 + z^2 - 2xy - 2xz - 2yz$  is the kinematical triangle Kallen function and

$$\begin{aligned} A_1 &= 2 \sin^2 \theta_l (H_{1/2,0}^2 + H_{-1/2,0}^2) + (1 - \cos \theta_l)^2 H_{1/2,1}^2 \\ & \quad + (1 + \cos \theta_l)^2 H_{-1/2,-1}^2, \\ A_2 &= 2 \cos^2 \theta_l (H_{1/2,0}^2 + H_{-1/2,0}^2) + \sin^2 \theta_l (H_{1/2,1}^2 + H_{-1/2,-1}^2) \\ & \quad - 4 \cos \theta_l (H_{1/2,1} H_{1/2,0} + H_{-1/2,1} H_{-1/2,0}) \\ & \quad + 2 (H_{1/2,1}^2 + H_{-1/2,1}^2). \end{aligned} \quad (6)$$

$\theta_l$  is the angle between momenta of the final hadron and the lepton in the  $q^2$  rest frame. The helicity amplitudes in Eq. (6),  $H_{\lambda_{\Lambda_c^*}, \lambda_{W^-}}^{VA}$ , can be expressed as a series functions of the form

factors defined in Eqs. (3) and (4),

$$\begin{aligned}
H_{\frac{1}{2},0}^V(1/2^+ \rightarrow 1/2^\pm) &= \frac{\sqrt{Q_\mp}}{\sqrt{q^2}} \left( M_\pm f(g)_1^V(q^2) \mp \frac{q^2}{M} f(g)_2^V(q^2) \right), \\
H_{\frac{1}{2},0}^A(1/2^+ \rightarrow 1/2^\pm) &= \frac{\sqrt{Q_\pm}}{\sqrt{q^2}} \left( M_\mp g(f)_1^A(q^2) \pm \frac{q^2}{M} g(f)_2^A(q^2) \right), \\
H_{\frac{1}{2},1}^V(1/2^+ \rightarrow 1/2^\pm) &= \sqrt{2Q_\mp} \left( f(g)_1^V(q^2) \mp \frac{M_\pm}{M} f(g)_2^V(q^2) \right), \\
H_{\frac{1}{2},1}^A(1/2^+ \rightarrow 1/2^\pm) &= \sqrt{2Q_\pm} \left( g(f)_1^A(q^2) \pm \frac{M_\mp}{M} g(f)_2^A(q^2) \right), \\
H_{\frac{1}{2},t}^V(1/2^+ \rightarrow 1/2^\pm) &= \frac{\sqrt{Q_\pm}}{\sqrt{q^2}} \left( M_\mp f(g)_1^V(q^2) \pm \frac{q^2}{M} f(g)_3^V(q^2) \right), \\
H_{\frac{1}{2},t}^A(1/2^+ \rightarrow 1/2^\pm) &= \frac{\sqrt{Q_\mp}}{\sqrt{q^2}} \left( M_\pm g(f)_1^A(q^2) \mp \frac{q^2}{M} g(f)_3^A(q^2) \right),
\end{aligned} \tag{7}$$

where  $Q_\pm$  is defined as  $Q_\pm = (M \pm M')^2 - q^2$  and  $M_\pm = M \pm M'$ .

The negative helicities for transitions involved final hadrons with  $J^P = 1/2^+$  and  $1/2^-$  can be obtained by

$$H_{-\lambda',-\lambda_W}^V = \mathcal{P}^V H_{\lambda',\lambda_W}^V, \quad H_{-\lambda',-\lambda_W}^A = \mathcal{P}^A H_{\lambda',\lambda_W}^A \tag{8}$$

with  $(\mathcal{P}^V, \mathcal{P}^A) = (+, -)$  and  $(-, +)$ , respectively. The total helicity amplitudes can be obtained by

$$H_{\lambda',\lambda_W} = H_{\lambda',\lambda_W}^V - H_{\lambda',\lambda_W}^A. \tag{9}$$

It is obvious that the form factors play important roles in the calculation of the semi-leptonic decays, which can be calculated by concrete models. In this work, we adopt light-front quark model, where the general expressions of  $\Lambda_b \rightarrow \Lambda_c^{(*)} (1/2^\pm)$  weak transitions are written as [24]

$$\begin{aligned}
&\langle \Lambda_c^{(*)} (1/2^+) (\bar{P}', J'_z) | \bar{c} \gamma^\mu (1 - \gamma_5) b | \Lambda_b (1/2^+) (\bar{P}, J_z) \rangle \\
&= \int \left( \frac{dx_1 d^2 \vec{k}_{1\perp}}{2(2\pi)^3} \right) \left( \frac{dx_2 d^2 \vec{k}_{2\perp}}{2(2\pi)^3} \right) \frac{\phi_{\Lambda_b}(x_i, \vec{k}_{i\perp}) \phi_{\Lambda_c^{(*)}}^*(x'_i, \vec{k}'_{i\perp})}{16 \sqrt{x_3 x'_3 M_0^3 M_0'^3}} \frac{\text{Tr}[(\bar{P}' - M'_0) \gamma_5 (\not{p}_1 + m_1) (\bar{P} + M_0) \gamma_5 (\not{p}_2 - m_2)]}{\sqrt{(e_1 + m_1)(e_2 + m_2)(e_3 + m_3)(e'_1 + m'_1)(e'_2 + m'_2)(e'_3 + m'_3)}} \\
&\quad \times \bar{u}(\bar{P}', J'_z) (\not{p}'_3 + m'_3) \gamma^\mu (1 - \gamma_5) (\not{p}_3 + m_3) u(\bar{P}, J_z),
\end{aligned} \tag{10}$$

$$\begin{aligned}
&\langle \Lambda_c^* (1/2^-) (\bar{P}', J'_z) | \bar{c} \gamma^\mu (1 - \gamma_5) b | \Lambda_b (1/2^+) (\bar{P}, J_z) \rangle \\
&= \int \left( \frac{dx_1 d^2 \vec{k}_{1\perp}}{2(2\pi)^3} \right) \left( \frac{dx_2 d^2 \vec{k}_{2\perp}}{2(2\pi)^3} \right) \frac{\phi_{\Lambda_b}(x_i, \vec{k}_{i\perp}) \phi_{\Lambda_c^*}^*(x'_i, \vec{k}'_{i\perp})}{16 \sqrt{3x_3 x'_3 M_0^3 M_0'^3}} \frac{\text{Tr}[(\bar{P}' - M'_0) \gamma_5 (\not{p}_1 + m_1) (\bar{P} + M_0) \gamma_5 (\not{p}_2 - m_2)]}{\sqrt{(e_1 + m_1)(e_2 + m_2)(e_3 + m_3)(e'_1 + m'_1)(e'_2 + m'_2)(e'_3 - m'_3)}} \\
&\quad \times \frac{\sum_i m'_i / m'_3}{\sum_i m'_i + M'_0} \bar{u}(\bar{P}', J'_z) \left( \not{K}' - \frac{m_3'^2 - \mu'^2}{2M'_0} \right) \gamma_5 (\not{p}'_3 + m'_3) \gamma^\mu (1 - \gamma_5) (\not{p}_3 + m_3) u(\bar{P}, J_z),
\end{aligned} \tag{11}$$

where  $K' = \frac{(m'_1 + m'_2) p'_3 - m'_3 (p_1 + p_2)}{m'_1 + m'_2 + m'_3}$  is the  $\lambda$ -mode momentum of the final hadron. And,  $\mu' = m'_1 m'_2 / m'_1 + m'_2$ ;  $\bar{P} = p_1 + p_2 + p_3$  and  $\bar{P}' = p_1 + p_2 + p'_3$  are the light-front momentum for initial or final hadrons respectively, considering  $p_1 = p'_1$  and  $p_2 = p'_2$  in the spectator model.  $\phi(x_i, \vec{k}_{i\perp})$  and  $\phi^*(x'_i, \vec{k}'_{i\perp})$  represent the wave functions for initial or final hadrons, respectively.

We follow Ref. [19], where they chosen a special gauge  $q^+ = 0$ , to get the form factors with  $V^+$ ,  $A^+$ ,  $\vec{q}_\perp \cdot \vec{V}$ ,  $\vec{q}_\perp \cdot \vec{A}$ ,  $\vec{n}_\perp \cdot \vec{V}$ , and  $\vec{n}_\perp \cdot \vec{A}$  by the way shown below. Firstly, multiply  $\sum_{J_z, J'_z} \delta_{J_z, J'_z}$ ,  $\sum_{J_z, J'_z} (\sigma^3)_{J_z, J'_z}$ ,  $\sum_{J_z, J'_z} (\vec{\sigma} \cdot \vec{q}_\perp)_{J_z, J'_z}$ ,  $\sum_{J_z, J'_z} (\vec{\sigma} \cdot \vec{q}_\perp \sigma^3)_{J_z, J'_z}$  onto both sides of Eq. (3) and Eq. (4), and then use Eq. (11) of Ref. [19] in the right side, use Eq. (10), Eq. (11) and Eq. (10) of Ref. [19] in the left side. Following the above steps we can finally obtain the concrete expressions for the involved form factors.

The expressions for the form factors describing  $\Lambda_b \rightarrow \Lambda_c^{(*)}(1/2^+)$  transitions are

$$\begin{aligned}
f_1^V(q^2) &= \int \mathcal{D}\mathcal{S} \frac{1}{8P^+P'^+} \text{Tr}[(\vec{P} + M_0)\gamma^+(\vec{P}' + M'_0)(\not{p}'_3 + m'_3)\gamma^+(\not{p}_3 + m_3)], \\
f_2^V(q^2) &= \int \mathcal{D}\mathcal{S} \frac{iM}{8P^+P'^+q^2} \text{Tr}[(\vec{P} + M_0)\sigma^{+\mu}q_\mu(\vec{P}' + M'_0)(\not{p}'_3 + m'_3)\gamma^+(\not{p}_3 + m_3)], \\
f_3^V(q^2) &= \frac{M}{M + M'} \left( f_1^V(q^2) \left(1 - \frac{2\vec{P} \cdot q}{q^2}\right) + \int \mathcal{D}\mathcal{S} \frac{1}{4\sqrt{P^+P'^+}q^2} \text{Tr}[(\vec{P} + M_0)\gamma^+(\vec{P}' + M'_0)(\not{p}'_3 + m'_3)\not{q}(\not{p}_3 + m_3)] \right), \\
g_1^A(q^2) &= \int \mathcal{D}\mathcal{S} \frac{1}{8P^+P'^+} \text{Tr}[(\vec{P} + M_0)\gamma^+\gamma_5(\vec{P}' + M'_0)(\not{p}'_3 + m'_3)\gamma^+\gamma_5(\not{p}_3 + m_3)], \\
g_2^A(q^2) &= \int \mathcal{D}\mathcal{S} \frac{-iM}{8P^+P'^+q^2} \text{Tr}[(\vec{P} + M_0)\sigma^{+\mu}q_\mu\gamma_5(\vec{P}' + M'_0)(\not{p}'_3 + m'_3)\gamma^+\gamma_5(\not{p}_3 + m_3)], \\
g_3^A(q^2) &= \frac{M}{M - M'} \left( g_1^A(q^2) \left(-1 + \frac{2\vec{P} \cdot q}{q^2}\right) + \int \mathcal{D}\mathcal{S} \frac{-1}{4\sqrt{P^+P'^+}q^2} \text{Tr}[(\vec{P} + M_0)\gamma^+\gamma_5(\vec{P}' + M'_0)(\not{p}'_3 + m'_3)\not{q}\gamma_5(\not{p}_3 + m_3)] \right)
\end{aligned} \tag{12}$$

with

$$\mathcal{D}\mathcal{S} = \frac{dx_1 d^2\vec{k}_{1\perp} dx_2 d^2\vec{k}_{2\perp}}{2(2\pi)^3 2(2\pi)^3} \frac{\phi^*(x'_i, \vec{k}'_{i\perp}) \phi(x_i, \vec{k}_{i\perp})}{16\sqrt{x_3 x'_3 M_0^3 M_0'^3}} \frac{\text{Tr}[(\vec{P}' - M'_0)\gamma_5(\not{p}_1 + m_1)(\vec{P} + M_0)\gamma_5(\not{p}_2 - m_2)]}{\sqrt{(e_1 + m_1)(e_2 + m_2)(e_3 + m_3)(e'_1 + m'_1)(e_2 + m'_2)(e_3 + m'_3)}}, \tag{13}$$

while the expressions for the form factors describing  $\Lambda_b \rightarrow \Lambda_c(1/2^-)$  transition are

$$\begin{aligned}
g_1^V(q^2) &= \int \mathcal{D}\mathcal{P} \frac{1}{8P^+P'^+} \text{Tr}[(\vec{P} + M_0)\gamma^+\gamma_5(\vec{P}' + M'_0) \left( \not{K}' - \frac{m_3'^2 - \mu'^2}{2M_0'} \right) \gamma_5(\not{p}'_3 + m'_3)\gamma^+(\not{p}_3 + m_3)], \\
g_2^V(q^2) &= \int \mathcal{D}\mathcal{P} \frac{-iM}{8P^+P'^+q^2} \text{Tr}[(\vec{P} + M_0)\sigma^{+\mu}q_\mu\gamma_5(\vec{P}' + M'_0) \left( \not{K}' - \frac{m_3'^2 - \mu'^2}{2M_0'} \right) \gamma_5(\not{p}'_3 + m'_3)\gamma^+(\not{p}_3 + m_3)], \\
g_3^V(q^2) &= \frac{M}{M + M'} \left( f_1^V(q^2) \left(1 - \frac{2\vec{P} \cdot q}{q^2}\right) \right. \\
&\quad \left. + \int \mathcal{D}\mathcal{P} \frac{1}{4\sqrt{P^+P'^+}q^2} \text{Tr}[(\vec{P} + M_0)\gamma^+\gamma_5(\vec{P}' + M'_0) \left( \not{K}' - \frac{m_3'^2 - \mu'^2}{2M_0'} \right) \gamma_5(\not{p}'_3 + m'_3)\not{q}(\not{p}_3 + m_3)] \right), \\
f_1^A(q^2) &= \int \mathcal{D}\mathcal{P} \frac{1}{8P^+P'^+} \text{Tr}[(\vec{P} + M_0)\gamma^+(\vec{P}' + M'_0) \left( \not{K}' - \frac{m_3'^2 - \mu'^2}{2M_0'} \right) \gamma_5(\not{p}'_3 + m'_3)\gamma^+\gamma_5(\not{p}_3 + m_3)], \\
f_2^A(q^2) &= \int \mathcal{D}\mathcal{P} \frac{iM}{8P^+P'^+q^2} \text{Tr}[(\vec{P} + M_0)\sigma^{+\mu}q_\mu(\vec{P}' + M'_0) \left( \not{K}' - \frac{m_3'^2 - \mu'^2}{2M_0'} \right) \gamma_5(\not{p}'_3 + m'_3)\gamma^+\gamma_5(\not{p}_3 + m_3)], \\
f_3^A(q^2) &= \frac{M}{M - M'} \left( g_1^A(q^2) \left(-1 + \frac{2\vec{P} \cdot q}{q^2}\right) \right. \\
&\quad \left. + \int \mathcal{D}\mathcal{P} \frac{-1}{4\sqrt{P^+P'^+}q^2} \text{Tr}[(\vec{P} + M_0)\gamma^+(\vec{P}' + M'_0) \left( \not{K}' - \frac{m_3'^2 - \mu'^2}{2M_0'} \right) \gamma_5(\not{p}'_3 + m'_3)\not{q}\gamma_5(\not{p}_3 + m_3)] \right)
\end{aligned} \tag{14}$$

with

$$\mathcal{D}\mathcal{P} = \frac{dx_1 d^2\vec{k}_{1\perp} dx_2 d^2\vec{k}_{2\perp}}{2(2\pi)^3 2(2\pi)^3} \frac{\phi^*(x'_i, \vec{k}'_{i\perp}) \phi(x_i, \vec{k}_{i\perp})}{16\sqrt{3x_3 x'_3 M_0^3 M_0'^3}} \frac{(\sum_i m'_i)/m'_3}{(M'_0 + \sum_i m'_i)} \frac{\text{Tr}[(\vec{P}' - M'_0)\gamma_5(\not{p}_1 + m_1)(\vec{P} + M_0)\gamma_5(\not{p}_2 - m_2)]}{\sqrt{(e_1 + m_1)(e_2 + m_2)(e_3 + m_3)(e'_1 + m'_1)(e_2 + m'_2)(e_3 - m'_3)}}. \tag{15}$$

The ones for  $\Lambda_c \rightarrow \Lambda^{(*)}(1/2^\pm)$  modes have the same expressions. Since the light-front quark model has been widely used for studying the weak transition form factors, we would not repeatedly introduce the explicit forms for this model here. One can turn to Refs. [16, 19, 21, 22, 24, 72–77] for detailed

introductions.

The spatial wave functions of these baryons involved in the discussed semi-leptonic decay are crucial input when calculating the form factors. In the previous works, the spatial wave functions were generally used in a simple harmonic oscilla-



tor forms with the oscillator parameter  $\beta$  [19, 21, 22, 24]. In this work, we adopted the exact spatial wave functions for the involved baryons with the help of the GEM, which will be introduced in the next subsection. This approach should be supported by the study of mass spectrum of baryon.

### B. The spatial wave function of these involved baryons

Different from former treatments [19, 21, 22, 24], in this work we adopt GEM to get the wave functions of baryons. As is known, baryons are formed by three constituent quarks in traditional constituent quark model. Different from meson, one baryon bound state is typical three-body system, and its wave function can be extracted by solving the three-body Schrodinger equation. In this work, we use the semi-relativistic potentials introduced by Godfrey and Isgur [78], which was applied by Capstick and Isgur to study baryon spectroscopy [79].

In the light quark sector, the relativistic effects in effective potential should be considered. Those effects are introduced by two ways in GI model. At the first step, the GI model introduces a smeared function, and thus the Hamiltonian depicted three-body bound system can be written as

$$\mathcal{H} = K + \sum_{i=1<j}^3 (S_{ij} + G_{ij} + V_{ij}^{\text{so}(s)} + V_{ij}^{\text{so}(v)} + V_{ij}^{\text{tens}} + V_{ij}^{\text{con}}), \quad (16)$$

where  $K$ ,  $S$ ,  $G$ ,  $V^{\text{so}(s)}$ ,  $V^{\text{so}(v)}$ ,  $V^{\text{tens}}$  and  $V^{\text{con}}$  stand for the kinetic energy, spin-independent linear confinement piece, Coulomb-like potential, scalar type-spin-orbit interaction, vector type-spin-orbit interaction, tensor potential and spin-dependent contact potential, respectively. They are written as [78–81]

$$K = \sum_{i=1,2,3} \sqrt{m_i^2 + p_i^2}, \quad (17)$$

$$S_{ij} = -\frac{3}{4} \left( br_{ij} \left[ \frac{e^{-\sigma^2 r_{ij}^2}}{\sqrt{\pi} \sigma r_{ij}} + \left( 1 + \frac{1}{2\sigma^2 r_{ij}^2} \right) \frac{2}{\sqrt{\pi}} \times \int_0^{\sigma r_{ij}} e^{-x^2} dx \right] \mathbf{F}_i \cdot \mathbf{F}_j + \frac{c}{3} \right), \quad (18)$$

$$G_{ij} = \sum_k \frac{\alpha_k}{r_{ij}} \left[ \frac{2}{\sqrt{\pi}} \int_0^{\tau_k r_{ij}} e^{-x^2} dx \right] \mathbf{F}_i \cdot \mathbf{F}_j, \quad (19)$$

for spin-independent terms with

$$\sigma^2 = \sigma_0^2 \left[ \frac{1}{2} + \frac{1}{2} \left( \frac{4m_i m_j}{(m_i + m_j)^2} \right)^4 + s^2 \left( \frac{2m_i m_j}{m_i + m_j} \right)^2 \right], \quad (20)$$

TABLE I: The parameters used in the GI model.

Parameters	Values	Parameters	Values
$m_u$ (GeV)	0.220	$\epsilon^{\text{so}(s)}$	0.448
$m_d$ (GeV)	0.220	$\epsilon^{\text{so}(v)}$	-0.062
$m_s$ (GeV)	0.419	$\epsilon^{\text{tens}}$	0.379
$m_c$ (GeV)	1.628	$\epsilon^{\text{con}}$	-0.142
$m_b$ (GeV)	4.977	$\sigma_0$ (GeV)	2.242
$b$ (GeV <sup>2</sup> )	0.142	$s$	0.805
$c$ (GeV)	-0.302		

and

$$V_{ij}^{\text{so}(s)} = -\frac{\mathbf{r}_{ij} \times \mathbf{p}_i \cdot \mathbf{S}_i}{2m_i^2} \frac{1}{r_{ij}} \frac{\partial S_{ij}}{r_{ij}} - \frac{\mathbf{r}_{ij} \times \mathbf{p}_j \cdot \mathbf{S}_j}{2m_j^2} \frac{1}{r_{ij}} \frac{\partial S_{ij}}{\partial r_{ij}},$$

$$V_{ij}^{\text{so}(v)} = \frac{\mathbf{r}_{ij} \times \mathbf{p}_i \cdot \mathbf{S}_i}{2m_i^2} \frac{1}{r_{ij}} \frac{\partial G_{ij}}{r_{ij}} + \frac{\mathbf{r}_{ij} \times \mathbf{p}_j \cdot \mathbf{S}_j}{2m_j^2} \frac{1}{r_{ij}} \frac{\partial G_{ij}}{r_{ij}} + \frac{\mathbf{r}_{ij} \times \mathbf{p}_i \cdot \mathbf{S}_i + \mathbf{r}_{ij} \times \mathbf{p}_j \cdot \mathbf{S}_j}{m_i m_j} \frac{1}{r_{ij}} \frac{\partial G_{ij}}{\partial r_{ij}},$$

$$V_{ij}^{\text{ten}} = -\frac{1}{m_i m_j} \left[ (\mathbf{S}_i \cdot \mathbf{r}_{ij})(\mathbf{S}_j \cdot \mathbf{r}_{ij}) - \frac{\mathbf{S}_i \cdot \mathbf{S}_j}{3} \right] \left( \frac{\partial^2 G_{ij}}{\partial r^2} - \frac{\partial G_{ij}}{r_{ij} \partial r_{ij}} \right),$$

$$V_{ij}^{\text{con}} = \frac{2\mathbf{S}_i \cdot \mathbf{S}_j}{3m_i m_j} \nabla^2 G_{ij},$$

for the spin-dependent terms, where,  $m_i$  and  $m_j$  are the mass of quark  $i$  and  $j$ , respectively.  $\langle \mathbf{F}_i \cdot \mathbf{F}_j \rangle = -2/3$  for quark-quark interaction.

At the second step, a general potential which relies on the center-of-mass of interacting quarks and momentum are made up for the loss of relativistic effects in the non-relativistic limit [78–82],

$$G_{ij} \rightarrow \left( 1 + \frac{p^2}{E_i E_j} \right)^{1/2} G_{ij} \left( 1 + \frac{p^2}{E_i E_j} \right)^{1/2}, \quad (21)$$

$$\frac{V_{ij}^k}{m_i m_j} \rightarrow \left( \frac{m_i m_j}{E_i E_j} \right)^{1/2 + \epsilon_k} \frac{V_{ij}^k}{m_i m_j} \left( \frac{m_i m_j}{E_i E_j} \right)^{1/2 + \epsilon_k}$$

with  $E_i = \sqrt{p^2 + m_i^2}$ , where subscript  $k$  was applied to distinguish the contributions from the contact, tensor, vector spin-orbit and scalar spin-orbit terms. In addition,  $\epsilon_k$  represents the relevant modification parameters, which are listed in Table I.

Now we illustrate the construction of baryon wave function. The total wave function is composed of color, flavor, space, and spin wave functions as

$$\Psi_{\mathbf{J}, \mathbf{M}_J} = \chi^c \left\{ \chi_{\mathbf{S}, \mathbf{M}_S}^s \psi_{\mathbf{L}, \mathbf{M}_L}^p \right\}_{\mathbf{J}, \mathbf{M}_J} \psi^f, \quad (22)$$

where  $\chi^c = \frac{1}{\sqrt{6}}(rgb - rbg + gbr - grb + brg - bgr)$  is the color wave function and is universal. The subscripts  $\mathbf{S}$ ,  $\mathbf{L}$  and  $\mathbf{J}$  are the total spin angular momentum, total orbital angular momentum and total angular momentum quantum numbers, respectively.  $\psi_{\mathbf{L}, \mathbf{M}_L}^p$  denotes the spatial wave function consisting of  $\rho$ -mode and  $\lambda$ -mode as

$$\psi_{\mathbf{L}, \mathbf{M}_L}^p(\vec{\rho}, \vec{\lambda}) = \left\{ \phi_{l_\rho, m_{l_\rho}}(\vec{\rho}) \phi_{l_\lambda, m_{l_\lambda}}(\vec{\lambda}) \right\}_{\mathbf{L}, \mathbf{M}_L}, \quad (23)$$

TABLE II: The spatial wave functions of  $\Lambda_b$ ,  $\Lambda_c^{(*)}(1/2^\pm)$  as well as  $\Lambda^{(*)}(1/2^\pm)$  with the GI model by the GEM. The Gaussian bases  $(n_\rho, n_\lambda)$  listed in the third column are arranged as:  $[(1, 1), (1, 2), \dots, (1, n_{\lambda_{max}}), (2, 1), (2, 2), \dots, (2, n_{\lambda_{max}}), \dots, (n_{\rho_{max}}, 1), (n_{\rho_{max}}, 2), \dots, (n_{\rho_{max}}, n_{\lambda_{max}})]$ . Here, we also listed the names of states, which are given in PDG, in the second column.

States	Name in PDG	Eigenvectors
$\Lambda_b(\frac{1}{2}^+)$	$\Lambda_b$	$[-0.0177, -0.0561, -0.0930, -0.0020, -0.0022, 0.0007, -0.0382, 0.0018, -0.0009, -0.0024, 0.0020, -0.0006, 0.0172, -0.3036, -0.2450, -0.0090, -0.0030, 0.0010, 0.0070, 0.0590, -0.3754, -0.0091, -0.0024, 0.0008, -0.0090, -0.0043, -0.0265, -0.1238, 0.0256, -0.0057, 0.0026, 0.0022, 0.0169, 0.0149, -0.0088, 0.0018]$
$\Lambda_c(\frac{1}{2}^+)$	$\Lambda_c^+$	$[-0.0162, -0.0404, -0.1010, -0.0174, 0.0003, 0.0001, -0.0321, -0.0094, -0.0024, -0.0027, 0.0019, -0.0005, 0.0163, -0.2232, -0.2985, -0.0527, 0.0045, -0.0007, 0.0002, 0.0701, -0.3035, -0.0831, 0.0127, -0.0027, -0.0054, -0.0095, -0.0129, -0.1277, 0.0183, -0.0042, 0.0018, 0.0024, 0.0135, 0.0186, -0.0085, 0.0016]$
$\Lambda_c(\frac{1}{2}^-)$	$\Lambda_c(2595)^+$	$[0.0044, 0.0227, 0.0983, 0.0423, -0.0049, 0.0010, 0.0149, -0.0018, 0.0083, 0.0016, -0.0011, 0.0003, -0.0065, 0.1155, 0.3076, 0.1148, -0.0139, 0.0030, 0.0021, -0.0485, 0.2750, 0.1689, -0.0283, 0.0067, 0.0037, 0.0011, 0.0136, 0.1510, -0.0104, 0.0026, -0.0013, 0.0005, -0.0131, -0.0266, 0.0080, -0.0015]$
$\Lambda_c^*(\frac{1}{2}^+)$	$\Lambda_c(2765)^+$	$[-0.0244, -0.0944, -0.127630, 0.1982, -0.0127, 0.0034, -0.0375, -0.0588, 0.0207, 0.0079, -0.0028, 0.0004, 0.0206, -0.4044, -0.4802, 0.5686, -0.0447, 0.0110, 0.0099, 0.0386, -0.2691, 0.5855, -0.0219, 0.0051, -0.0080, -0.0099, -0.1144, 0.3734, 0.0859, -0.0156, 0.0014, 0.0089, 0.0311, -0.0673, 0.0101, 0.0002]$
$\Lambda(\frac{1}{2}^+)$	$\Lambda$	$[0.0171, 0.0239, 0.0847, 0.0412, 0.0035, -0.0005, 0.0373, -0.0047, 0.0106, 0.0004, -0.0013, 0.0006, -0.0192, 0.1969, 0.2244, 0.1544, -0.0024, 0.0017, 0.0014, -0.0693, 0.2616, 0.1231, 0.0116, -0.0003, 0.0041, 0.0115, -0.0091, 0.1469, -0.0115, 0.0038, -0.0016, -0.0021, -0.0071, -0.0248, 0.0090, -0.0022]$
$\Lambda(\frac{1}{2}^-)$	$\Lambda(1405)$	$[0.0058, 0.0145, 0.0715, 0.0639, 0.0019, 0.0002, 0.0193, -0.0075, 0.0074, 0.0028, -0.0015, 0.0004, -0.0101, 0.1087, 0.2125, 0.1904, 0.0020, 0.0013, 0.0027, -0.0469, 0.2260, 0.2215, -0.0009, 0.0029, 0.0022, 0.0061, -0.0113, 0.1742, 0.0127, -0.0007, -0.0010, -0.0005, -0.0054, -0.0329, 0.0063, -0.0012]$
$\Lambda^*(\frac{1}{2}^+)$	$\Lambda(1600)$	$[0.0310, 0.0424, 0.1590, -0.1262, -0.0378, 0.0031, 0.0429, 0.0480, -0.0085, -0.0117, 0.0011, 0.0000, -0.0119, 0.2645, 0.5786, -0.2742, -0.1134, 0.0120, -0.0001, -0.0639, 0.2197, -0.4162, -0.1299, 0.0128, 0.0063, 0.0065, 0.1069, -0.3538, -0.2064, 0.0247, -0.0012, -0.0062, -0.0280, 0.0514, 0.0050, -0.0022]$

where the subscripts  $\mathbf{l}_\rho$  and  $\mathbf{l}_\lambda$  are the orbital angular momentum for  $\rho$  and  $\lambda$ -mode, respectively. In this paper, the internal Jacobi coordinates are chosen as

$$\vec{\rho} = \vec{r}_1 - \vec{r}_2, \quad \vec{\lambda} = \vec{r}_3 - \frac{m_1 \vec{r}_1 + m_2 \vec{r}_2}{m_1 + m_2}. \quad (24)$$

Note that we only use one channel here. It is suitable for singly heavy baryons while it is an approximation for light baryons.

The Rayleigh-Ritz variational principle is used in this work to solve the three-body Schrodinger equation

$$\mathcal{H}\Psi_{J,M_J} = E\Psi_{J,M_J}, \quad (25)$$

and thus we can obtain the eigenvalues  $E$ , and the spatial wave functions. The Gaussian basis [83–85]

$$\phi_{n,l,m}^G(\vec{r}) = \phi_{n,l}^G(r)Y_{l,m}(\hat{r}), \quad (26)$$

are used to expand the spatial wave function, where  $n = 1, 2, \dots, n_{max}$  with a freedom parameter  $n_{max}$  which should be chosen from positive integers, and the Gaussian size parameters  $v_n$  are settled as a geometric progression as

$$v_n = 1/r_n^2, \quad r_n = r_{min} a^{n-1} \quad (27)$$

with

$$a = \left( \frac{r_{max}}{r_{min}} \right)^{\frac{1}{n_{max}-1}}.$$

Using the parameters collected in Table I as input, we can obtain the masses<sup>1</sup> and spatial wave functions of baryons. Additionally, in our calculation the values of  $\rho_{min}$  and  $\rho_{max}$  are chosen as 0.2 fm and 2.0 fm, respectively, and  $n_{\rho_{max}} = 6$ . For  $\lambda$ -mode, we also use the same Gaussian sized parameters. In Table II, we collect the numerical spatial wave functions of bottom and charmed baryons, and the ground and excited states of  $\Lambda$  involved in these discussed semi-leptonic decays. It should be noted that the spatial wave functions obtained in this work are based on a systematic analysis of all the related  $\Lambda_b$ ,  $\Lambda_c^{(*)}$  and  $\Lambda^{(*)}$  baryons.

<sup>1</sup> For the ground states, the estimated masses are 1131 MeV, 2286 MeV and 5621 MeV for  $\Lambda$ ,  $\Lambda_c$  and  $\Lambda_b$ , respectively, which are close to the experimental data 1116 MeV, 2286.46  $\pm$  0.14 MeV and 5619.60  $\pm$  0.17 MeV [14]. Besides, the estimated masses for  $\Lambda_c(1/2^-)$  and  $\Lambda_c^*(1/2^+)$  are 2615 MeV and 2765 MeV, respectively, which can also repeat the experimental data 2592.25  $\pm$  0.28 and 2766.6  $\pm$  2.4 MeV [14]. While for the (*uds*)-type  $\Lambda^*$  resonances, the estimations for  $\Lambda(1/2^-)$  and  $\Lambda^*(1/2^+)$  are 1517 MeV and 1679 MeV, respectively, which mark differences compared to  $\Lambda(1405)$ 's 1405.1<sup>+1.3</sup><sub>-1.0</sub> MeV and  $\Lambda(1600)$ 's (1570 ~ 1630) MeV [14]. It is worthy to mention that there is only one channel [84, 85] used in this work. The big differences indicate more complicated structures for light baryons. For  $\Lambda(1405)$ , our estimation is roughly consistent with the constituent quark model [38, 84], while its structure is still a mystery need to be understood. More discussions on this resonance can be get in Refs. [86–89] and the references therein.

TABLE III: The form factors for  $\Lambda_b \rightarrow \Lambda_c^{(*)}$  in this work. We use a three parameter form as illustrated in Eq. (28) for these form factors.

	$F(0)$	$F(q_{max}^2)$	$b_1$	$b_2$
$\Lambda_b \rightarrow \Lambda_c \left(\frac{1}{2}^+\right)$				
$f_1^V$	0.503	1.012	0.713	0.141
$f_2^V$	-0.121	-0.286	1.134	0.399
$f_3^V$	-0.044	-0.108	1.158	0.324
$g_1^A$	0.494	0.977	0.677	0.142
$g_2^A$	-0.024	-0.053	0.980	0.352
$g_3^A$	-0.146	-0.364	1.287	0.567
$\Lambda_b \rightarrow \Lambda_c \left(\frac{1}{2}^-\right)$				
$g_1^V$	0.389	0.557	0.152	0.330
$g_2^V$	-0.326	-0.709	1.417	0.695
$g_3^V$	-0.546	-1.227	1.477	0.663
$f_1^A$	0.435	0.695	0.448	0.139
$f_2^A$	-0.383	-0.796	1.268	0.544
$f_3^A$	-0.445	-0.974	1.444	0.756
$\Lambda_b \rightarrow \Lambda_c^* \left(\frac{1}{2}^+\right)$				
$f_1^V$	0.196	0.183	-1.192	2.051
$f_2^V$	-0.066	-0.076	-0.334	1.281
$f_3^V$	-0.109	-0.200	1.132	0.387
$g_1^A$	0.187	0.169	-1.315	2.239
$g_2^A$	-0.083	-0.166	1.296	0.077
$g_3^A$	-0.088	-0.116	0.149	0.899

#### IV. NUMERICAL RESULTS

##### A. The calculated form factors

In this subsection, we present our results for the form factors of  $\Lambda_b \rightarrow \Lambda_c^{(*)}(1/2^\pm)$  and  $\Lambda_c \rightarrow \Lambda^{(*)}(1/2^\pm)$  transitions. The mass of baryons we used in our calculation are cited from Ref. [14], and the spatial wave functions are obtained from GEM. The form factors obtained in section II are calculated out in space-like region, so we need to expand them to time-like region. We would use the dipole parametrization to obtain our form factors in physical region. The concrete expression reads as [19, 22]

$$F(q^2) = \frac{F(0)}{(1 - q^2/M^2)(1 - b_1 q^2/M^2 + b_2 (q^2/M^2)^2)}, \quad (28)$$

where  $b_1$  and  $b_2$  are two parameters needed to be fitted.

With the spatial wave functions for  $\Lambda_Q^{(*)}$ , we can obtain the form factors numerically in the framework of light-front quark model. In this way, we avoid the effective  $\beta$  parameters [19–21, 24, 90, 91], and all the free parameters can be fixed by fitting the mass spectra of baryons. The parameters for the extended form factors are collected in Table III and IV for  $\Lambda_b \rightarrow \Lambda_c^{(*)}(1/2^\pm)$  and  $\Lambda_c \rightarrow \Lambda^{(*)}(1/2^\pm)$  transitions, respectively.

The form factors for  $\Lambda_b \rightarrow \Lambda_c(1/2^+, 2286)$  transition can be worked out with the help of Eq. (10). The  $q^2$  dependence of  $f_{1,2,3}^V$  and  $g_{1,2,3}^A$  for this transition are plotted in the first panel of Fig. 2, and the fitting parameters in Eq. (28) are listed in Table III. In heavy quark limit (HQL), the corresponding

TABLE IV: The form factors for  $\Lambda_c \rightarrow \Lambda^{(*)}$  in this work. We use a three parameter form as illustrated in Eq. (28) for these form factors.

	$F(0)$	$F(q_{max}^2)$	$b_1$	$b_2$
$\Lambda_c \rightarrow \Lambda \left(\frac{1}{2}^+\right)$				
$f_1^V$	0.706	1.022	0.279	0.143
$f_2^V$	-0.362	-0.580	0.651	0.252
$f_3^V$	-0.286	-0.489	0.854	0.232
$g_1^A$	0.624	0.854	0.094	0.216
$g_2^A$	-0.113	-0.192	0.788	0.051
$g_3^A$	-0.598	-1.065	1.067	0.601
$\Lambda_c \rightarrow \Lambda \left(\frac{1}{2}^-\right)$				
$g_1^V$	0.463	0.484	-0.562	1.130
$g_2^V$	-0.410	-0.498	0.804	1.623
$g_3^V$	-1.452	-1.803	1.037	1.998
$f_1^A$	0.629	0.708	0.049	0.658
$f_2^A$	-0.557	-0.667	0.607	0.788
$f_3^A$	-0.749	-0.917	0.858	1.444
$\Lambda_c \rightarrow \Lambda^* \left(\frac{1}{2}^+\right)$				
$f_1^V$	0.194	0.169	-2.811	6.962
$f_2^V$	-0.106	-0.093	-2.677	7.559
$f_3^V$	-0.384	-0.419	0.311	1.366
$g_1^A$	0.131	0.105	-3.998	11.522
$g_2^A$	-0.226	-0.247	0.348	1.947
$g_3^A$	-0.350	-0.356	-0.598	3.307

transition matrix element can be rewritten as [11, 12, 92]

$$\langle \Lambda_c(v', s') | \bar{c}_\nu \Gamma b_\nu | \Lambda_b(v, s) \rangle = \zeta(\omega) \bar{u}(v', s') \Gamma u(v, s), \quad (29)$$

at the leading order in the heavy quark expansion, so that the form factors have more simpler behaviors as

$$\begin{aligned} f_1^V(q^2) &= g_1^A(q^2) = \zeta(\omega), \\ f_2^V &= f_3^V = g_2^A = g_3^A = 0, \end{aligned} \quad (30)$$

where  $\omega = v \cdot v' = (M^2 + M'^2 - q^2)/(2MM')$  while  $v' = p'/M'$  and  $v = p/M$  are the four-velocities for  $\Lambda_c$  and  $\Lambda_b$ , respectively.  $\zeta(\omega)$  is the so-called Isgur-Wise function (IWF) and usually expressed as a Taylor series expansion as [94]

$$\zeta(\omega) = 1 - \rho^2(\omega - 1) + \frac{\sigma^2}{2}(\omega - 1)^2 + \dots, \quad (31)$$

where  $\rho^2 = -\frac{d\zeta(\omega)}{d\omega}|_{\omega=1}$  and  $\sigma^2 = \frac{d^2\zeta(\omega)}{d\omega^2}|_{\omega=1}$  are the two important parameters for depicting the IWF. The most obvious character is in the point  $q^2 = q_{max}^2$  (or  $\omega = 1$ ),

$$f_1^V(q_{max}^2) = g_1^A(q_{max}^2) = \zeta(1) = 1.$$

It provides one strong restriction for our results. Either  $f_1^V(q_{max}^2) = 1.012$  or  $g_1^A(q_{max}^2) = 0.977$  in our results satisfies the above restriction. Besides, we can easily see that  $f_1^V$  and  $g_1^A$  are very close to each other, and dominate over  $f_{2,3}^V$  and  $g_{2,3}^A$ . These results satisfy the predictions of the heavy quark effective theory. At the mean time, we obtain the  $\rho^2$  and  $\sigma^2$  in Eq. (31), by fitting  $\zeta(\omega)$  from  $f_1^V(q^2)$  and  $g_1^A(q^2)$ . The



TABLE V: Our results for the IWF's shape parameters of  $\Lambda_b \rightarrow \Lambda_c$  transition. The superscripts [a] and [b] in the second and third rows represent the fitting of  $f_1^V$  and  $g_1^A$  respectively. In Ref. [58], they listed various theoretical predictions of  $\rho^2$  in Table 3 and we would not list those here repeatedly.

	$\rho^2$	$\sigma^2$
This work <sup>[a]</sup>	1.68	2.48
This work <sup>[b]</sup>	1.90	3.53
RQM [54]	1.51	4.06
QCDSR [60]	$1.35 \pm 0.13$	
LQCD [67]	$1.2^{+0.8}_{-1.1}$	
DELPHI [93]	$2.03 \pm 0.46^{+0.72}_{-1.00}$	
LHCb [94]	$1.63 \pm 0.07$	$2.16 \pm 0.34$

comparison with other theoretical predictions and the fitting of experimental data are listed in Table V. The slope parameter  $\rho^2$ , either from fitting  $f_1^V$  or  $g_1^A$ , is close to the results from DELPHI [93] and LHCb [94]. The parameter  $\sigma^2$  from  $g_1^A(q^2)$  is slightly greater than the measurement of LHCb Collaboration, while the one from  $f_1^V(q^2)$  is well agreed with the measurement.

For  $\Lambda_b \rightarrow \Lambda_c(1/2^-, 2595)$  transition, the  $q^2$  dependence of  $g_1^V$  and  $f_{1,2,3}^A$  for this transition are plotted in the second panel of Fig. 2. Similarly, the corresponding transition matrix element can be simplified and be rewritten as [19]

$$\langle \Lambda_c^*(1/2^-)(v') | \bar{c}_v \Gamma b_v | \Lambda_b(v) \rangle = \frac{\sigma(\omega)}{\sqrt{3}} \bar{u}(v') \gamma_5 (\not{v} + v \cdot \not{v}) \Gamma u(v), \quad (32)$$

in HQL. At the mean time, the form factors can be simplified as

$$\begin{aligned} g_1^V(q^2) &= f_1^A(q^2) = \left( \omega - \frac{M'}{M} \right) \frac{\sigma(\omega)}{\sqrt{3}}, \\ g_2^V(q^2) &= g_3^V(q^2) = f_2^A(q^2) = f_3^A(q^2) = -\frac{\sigma(\omega)}{\sqrt{3}}. \end{aligned} \quad (33)$$

When comparing our results with the predictions of heavy quark limit, we can draw the conclusion that our results match the main requirements of the above analysis with: 1.  $g_1^V$  is close to  $f_1^A$ , while  $g_{2,3}^V$  and  $f_{2,3}^A$  are close to each others. 2.  $f_1^A/f_{2,3}^A$  and  $f_1^V/f_{2,3}^V$  roughly close to  $(M' - M)/M$  at  $q^2 = q_{max}^2$ .

For  $\Lambda_b \rightarrow \Lambda_c^*(1/2^+, 2765)$  transition, the  $q^2$  dependence of  $f_{1,2,3}^V$  and  $g_{1,2,3}^A$  are plotted in the third panel of Fig. 2. The HQL expects  $f_1^V = g_1^A = 0$  at  $q^2 = q_{max}^2$ , because the wave functions of the low-lying  $\Lambda_b$  and the radial excited state  $\Lambda_c^*(2765)$  are orthogonal [19]. Evidently our results embody this character according to Fig. 2 and Table III.

For  $\Lambda_c \rightarrow \Lambda(1/2^+, 1116)$  form factors, The  $q^2$  dependence of  $f_{1,2,3}^V$  and  $g_{1,2,3}^A$  are plotted in the fourth panel of Fig. 2. One interesting prediction from heavy quark symmetry at  $q^2 = 0$  is that the daughter  $\Lambda$  baryon is predicted to emerge 100% polarized, with the decay asymmetry parameter  $\alpha_{q^2=0} = -1$ . Our result of  $-0.99$  is very close to the prediction. Besides, the mean value of the polarization  $\langle \alpha \rangle$  has been measured as  $-0.86 \pm 0.03 \pm 0.02$  by CLEO with high precision [95]. Our result of  $-0.87$  is well consistent with the above experiment.

As the form factors depicted  $\Lambda_c \rightarrow \Lambda(1/2^-, 1P)$  and  $\Lambda_c \rightarrow \Lambda^*(1/2^+, 2S)$  transitions, we also plot the  $q^2$  dependence of  $f_{1,2,3}$  and  $g_{1,2,3}$  in the fifth and sixth panels of Fig. 2. Without enough information to test these channels, we expect more experiments and more theories, especially the LQCD, may bring us the crucial breakthroughs in the future.

At last, we list our results for form factors of  $\Lambda_b \rightarrow \Lambda_c$  and  $\Lambda_c \rightarrow \Lambda$  transitions at  $q^2 = 0$  in Table VI and compare with other approaches. The calculations in Refs. [19, 20, 24, 25] were based on the light-front quark model. In more detail, Ref. [19] worked in the standard light-front quark model and diquark picture while Ref. [24] worked in the triquark picture. Refs. [20, 25] used covariant light-front quark model. A covariant consistent quark model was used in Ref. [55] and a RQM was used in Ref. [53]. Besides, the LQCDs' results [69, 71] are also listed here. We can see that our results are slightly greater than other theoretical predictions but still consistent with the restriction of LQCD [69, 71]. These form factors are important out of the ordinary for helping us to understand the weak decays and search for the undiscovered semi-leptonic channels. We expect more theoretical and experimental data for testing these results ulteriorly.

These transition form factors would be useful as inputs not only in the studies of semi-leptonic decays as to be shown in the following subsection, but also in the non-leptonic decays of  $\Lambda_b$  and  $\Lambda_c$  [98–112].

## B. Numerical results of the semi-leptonic decays observables

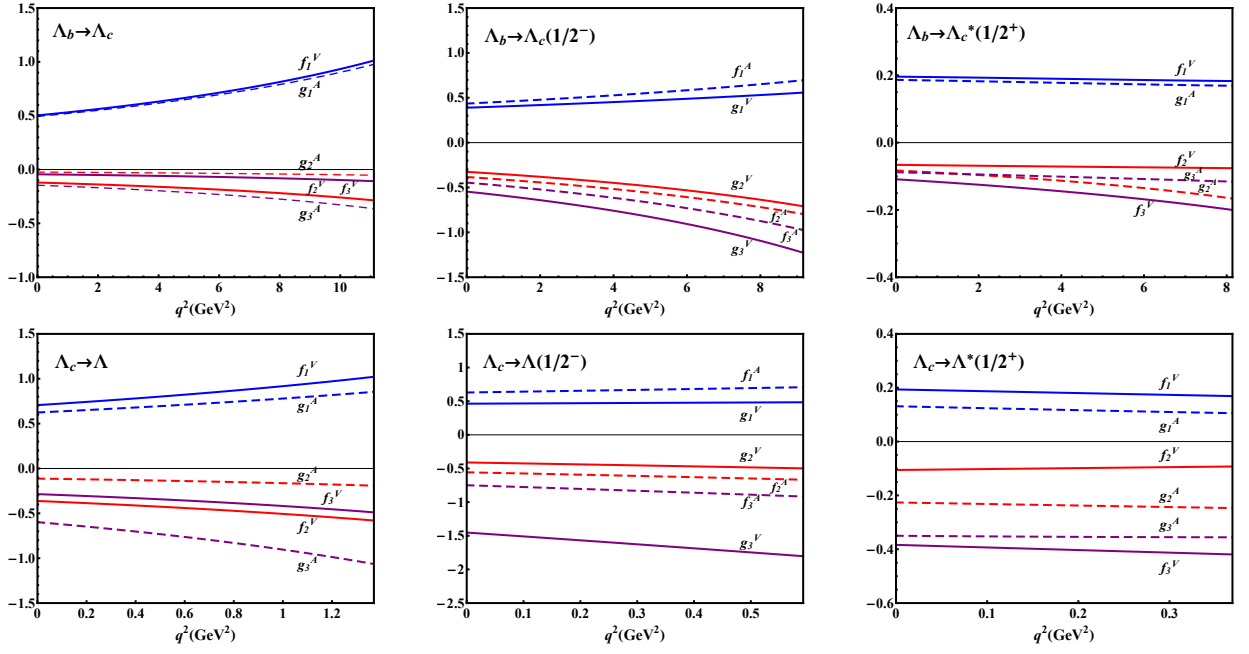
In order to calculate the physical observables in semi-leptonic process, we adopt helicity formalism. The baryon and lepton masses used in this paper are collected from the PDG [14], as well as  $\tau_{\Lambda_b} = 1.470$  ps. Besides,  $\tau_{\Lambda_c^*} = 203.5$  fs [113]. The CKM matrix elements are chosen as  $V_{cs} = 0.987$  and  $V_{cb} = 0.041$  [14].

The  $q^2$  dependence of differential decay widths of  $\Lambda_b \rightarrow \Lambda_c^{(*)}(1/2^\pm) \ell^- \nu_\ell$  and  $\Lambda_c \rightarrow \Lambda^{(*)}(1/2^\pm) \ell^- \nu_\ell$  processes, which can be obtained by integrating  $\theta_\ell$ , are shown in Fig. 3. At the meantime we list the branching fractions in Table VII, and compare our results with the data from experiment or LQCD.

It is obvious that our predictions for  $\mathcal{B}(\Lambda_b \rightarrow \Lambda_c e^- \nu_e (\mu^- \nu_\mu))$  are consistent with the experimental data while slightly greater than the LQCDs' results. As for the  $\tau$ -one, it is slightly over the upper limit of LQCD but tallies with Ref. [55] and Ref. [53].  $\mathcal{B}(\Lambda_c \rightarrow \Lambda e^+ \nu_e (\mu^+ \nu_\mu))$  is consistent with either the LQCD's or the BESIII's results. In 2009, the CDF Collaboration reported their estimation for  $\mathcal{B}(\Lambda_b \rightarrow \Lambda_c(2595) \mu^- \nu_\mu) = 0.9\%$  with almost 50% uncertainty. This is the only experimental data for excited channels. Our prediction for this one is near 1.8%, which is about two times of the superior limit for the current data. This demands us more information, in particular the form factors and the absolute branching rates by further experiment, on these channels. While for  $\Lambda_c^*(1/2^+)$  and  $\Lambda(1/2^-)$  channels, considering that our predictions for the  $e$  and  $\mu$ -modes are up to a few thousand of magnitude, we would like to take a positive attitude to discovering them in the futuristic experiments. These

TABLE VI: Theoretical predictions for the form factors  $f_{1,2}^V(0)$  and  $g_{1,2}^A(0)$  of  $\Lambda_b \rightarrow \Lambda_c$  and  $\Lambda_c \rightarrow \Lambda$  at  $q^2 = 0$  in different approaches.

	$f_1^V(0)$	$f_2^V(0)$	$g_1^A(0)$	$g_2^A(0)$
$\Lambda_b \rightarrow \Lambda_c$				
This work	0.503	-0.121	0.494	-0.024
LFQM [19]	$0.474^{+0.069}_{-0.072}$	$-0.109^{+0.019}_{-0.021}$	$0.468^{+0.067}_{-0.007}$	$0.051^{+0.008}_{-0.012}$
LFQM [20]	$0.500^{+0.028}_{-0.031}$	$-0.098^{+0.005}_{-0.004}$	$0.509^{+0.029}_{-0.031}$	$-0.014^{+0.001}_{-0.001}$
LFQM [24]	0.488	-0.180	0.470	-0.0479
RQM [53]	0.526	-0.137	0.505	0.027
CCQM [55]	0.549	-0.110	0.542	-0.018
LQCD [71]	$0.418 \pm 0.161$	$-0.100 \pm 0.055$	$0.378 \pm 0.102$	$-0.004 \pm 0.002$
$\Lambda_c \rightarrow \Lambda$				
This work	0.706	-0.362	0.624	-0.113
LFQM [23]	0.468	-0.222	0.407	-0.035
LFQM [25]	$0.67 \pm 0.01$	$-0.76 \pm 0.02$	$0.59 \pm 0.01$	$(1.59 \pm 0.05) \times 10^{-3}$
LCSR[36]	0.517	-0.123	0.517	0.123
CCQM [41]	0.511	-0.289	0.466	0.025
LQCD [69]	$0.647 \pm 0.122$	$-0.310 \pm 0.075$	$0.577 \pm 0.076$	$0.001 \pm 0.048$
LCSR [96]	0.449	-0.193	0.449	0.193
RQM [97]	0.700	-0.295	0.488	0.135

FIG. 2: The  $q^2$  dependence of form factors of  $\Lambda_b \rightarrow \Lambda_c^{(*)}(1/2^\pm)$  and  $\Lambda_c \rightarrow \Lambda^{(*)}(1/2^\pm)$  transitions, in which the solid and dashed lines represent the vector or pseudoscalar-types form factors respectively, while the blue, red and purple lines (both solid and dashed) represent the  $i$ -th form factors denoted by the subscripts respectively for each types.

decays can furnish a unique platform for studying the nature of the involved excited hadron states ulteriorly.

we briefly estimate the contributions from ground states, and obtain

$$\frac{\mathcal{B}(\Lambda_b \rightarrow \Lambda_c \ell^- \nu_\ell)}{\sum \mathcal{B}(\Lambda_b \rightarrow \Lambda_c^{(*)} \ell^- \nu_\ell)} \approx 0.77, \quad (34)$$

$$\frac{\mathcal{B}(\Lambda_c \rightarrow \Lambda \ell^+ \nu_\ell)}{\sum \mathcal{B}(\Lambda_c \rightarrow \Lambda^{(*)} \ell^+ \nu_\ell)} \approx 0.93,$$

with  $\ell = e$  or  $\mu$ . It indicates the decays to ground state

account for a great proportion in corresponding  $\Lambda_b$  and  $\Lambda_c$  semi-leptonic channels, which is consistent with the BESIII measurements of  $\mathcal{B}(\Lambda_c \rightarrow \Lambda e^+ \nu_e)/\mathcal{B}(\Lambda_c \rightarrow e^+ X) = (91.9 \pm 13.6)\%$ .

Besides other important physical observables, e.g. the leptonic forward-backward asymmetry ( $A_{FB}$ ), the final hadron polarization ( $P_B$ ) and the lepton polarization ( $P_l$ ) are also explored. Their characters dependant on  $q^2$  are shown in Figs. 4, 5 and 6, respectively. Their mean values are also listed in

TABLE VII: Our results for the absolute branching fractions  $\mathcal{B}(\Lambda_b \rightarrow \Lambda_c^{(*)} \ell^- \nu_\ell)$  with  $\ell^- = e^-, \mu^-, \tau^-$  and  $\mathcal{B}(\Lambda_c \rightarrow \Lambda^{(*)} \ell^+ \nu_\ell)$  with  $\ell^+ = e^+, \mu^+$ . The numbers out of the brackets are our predictions, while the ones in the brackets are the referential numbers with the superscript [exp] and [LQCD] denoting the data which comes from experiments [4, 6, 14, 95] or LQCD [69, 71], respectively. All the values are at the level of percent (%).

	$\Lambda_b \rightarrow \Lambda_c^{(*)} \ell \nu_\ell$			$\Lambda_c \rightarrow \Lambda^{(*)} \ell \nu_\ell$		
	$\Lambda_c \left(\frac{1}{2}^+\right)$	$\Lambda_c \left(\frac{1}{2}^-\right)$	$\Lambda_c^* \left(\frac{1}{2}^+\right)$	$\Lambda \left(\frac{1}{2}^+\right)$	$\Lambda \left(\frac{1}{2}^-\right)$	$\Lambda^* \left(\frac{1}{2}^+\right)$
$\ell = e$	6.46 ( $6.2_{-1.3}^{+1.4}$ [exp], $5.49 \pm 0.34$ [LQCD])	1.74	0.21	4.04 ( $3.63 \pm 0.43$ [exp], $3.80 \pm 0.22$ [LQCD])	0.31	0.007
$\ell = \mu$	6.44 ( $6.2_{-1.3}^{+1.4}$ [exp], $5.49 \pm 0.34$ [LQCD])	( $0.79_{-0.35}^{+0.40}$ [exp])	0.21	3.90 ( $3.49 \pm 0.46$ [exp], $3.69 \pm 0.22$ [LQCD])	0.28	0.005
$\ell = \tau$	1.97 ( $1.57 \pm 0.08$ [LQCD])	0.24	0.02	-	-	-

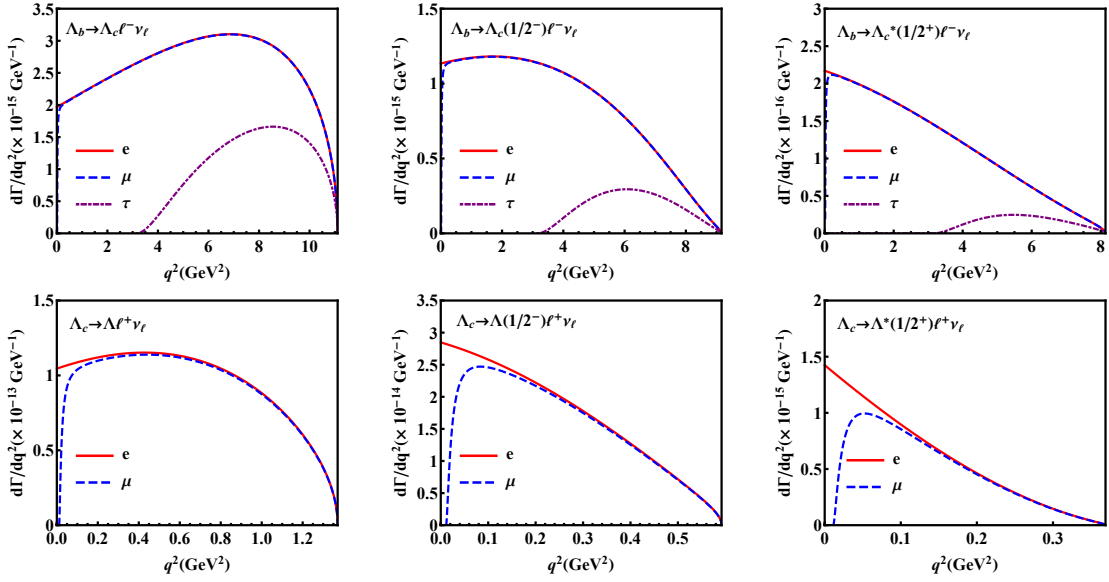


FIG. 3: The  $q^2$  dependence of differential decay widths for  $\Lambda_b \rightarrow \Lambda_c^{(*)} \ell^- \nu_\ell$  semi-leptonic decays with  $\ell^- = e^-$  (red solid line),  $\mu^-$  (blue dashed line),  $\tau^-$  (purple dot dashed line) and for  $\Lambda_c \rightarrow \Lambda^{(*)} \ell^+ \nu_\ell$  semi-leptonic decays with  $\ell^+ = e^+$  (red solid line),  $\mu^+$  (blue dashed line).

Table VIII. These parameters are defined as [114]

$$A_{FB}(q^2) = \frac{\int_0^1 \frac{d\Gamma}{dq^2 d\cos\theta_\ell} d\cos\theta_\ell - \int_{-1}^0 \frac{d\Gamma}{dq^2 d\cos\theta_\ell} d\cos\theta_\ell}{\int_0^1 \frac{d\Gamma}{dq^2 d\cos\theta_\ell} d\cos\theta_\ell + \int_{-1}^0 \frac{d\Gamma}{dq^2 d\cos\theta_\ell} d\cos\theta_\ell}, \quad (35)$$

$$P_B(q^2) = \frac{d\Gamma^{\lambda_2=1/2}/dq^2 - d\Gamma^{\lambda_2=-1/2}/dq^2}{d\Gamma/dq^2}, \quad (36)$$

$$P_\ell(q^2) = \frac{d\Gamma^{\lambda_\ell=1/2}/dq^2 - d\Gamma^{\lambda_\ell=-1/2}/dq^2}{d\Gamma/dq^2}, \quad (37)$$

respectively, where

$$\frac{d\Gamma^{\lambda_2=1/2}}{dq^2} = \frac{4m_l^2}{3q^2} \left( H_{1/2,1}^2 + H_{1/2,0}^2 + 3H_{1/2,t}^2 \right) + \frac{8}{3} \left( H_{1/2,0}^2 + H_{1/2,1}^2 \right), \quad (38)$$

$$\frac{d\Gamma^{\lambda_2=-1/2}}{dq^2} = \frac{4m_l^2}{3q^2} \left( H_{-1/2,-1}^2 + H_{-1/2,0}^2 + 3H_{-1/2,t}^2 \right) + \frac{8}{3} \left( H_{-1/2,-1}^2 + H_{-1/2,0}^2 \right), \quad (39)$$

$$\frac{d\Gamma^{\lambda_\ell=1/2}}{dq^2} = \frac{m_l^2}{q^2} \left[ \frac{4}{3} \left( H_{1/2,1}^2 + H_{1/2,0}^2 + H_{-1/2,-1}^2 + H_{-1/2,0}^2 \right) + 4 \left( H_{1/2,t}^2 + H_{-1/2,t}^2 \right) \right], \quad (40)$$

$$\frac{d\Gamma^{\lambda_\ell=-1/2}}{dq^2} = \frac{8}{3} \left( H_{1/2,1}^2 + H_{1/2,0}^2 + H_{-1/2,-1}^2 + H_{-1/2,0}^2 \right). \quad (41)$$

In Fig. 4, the leptonic forward-backward asymmetry  $F_{FB}$  always changes its sign at a  $q^2$  value which is associated with the mass of lepton. This character is consistent with Refs. [41, 53, 65]. In Fig. 5, the hadron polarization always vary from  $P_B = -1$  to  $P_B = 0$  as the  $q^2$  increasing from 0 to  $q_{\max}^2$ . The non-monotone behavior of  $\Lambda_b \rightarrow \Lambda_c(1/2^-) \ell^- \nu_\ell$

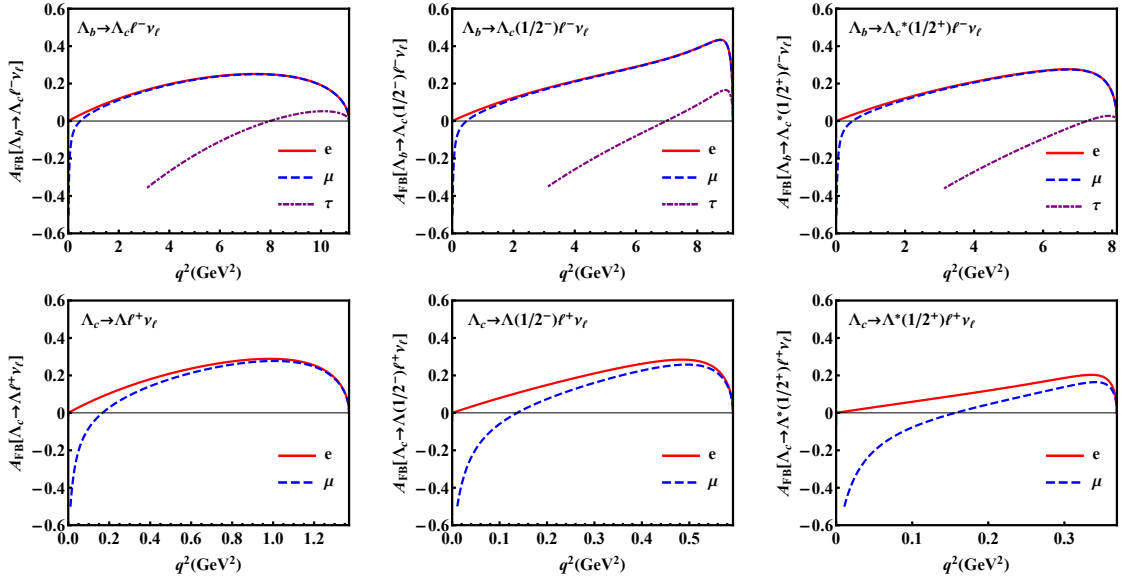


FIG. 4: The  $q^2$  dependence of lepton forward-backward asymmetry ( $A_{FB}$ ) for  $\Lambda_b \rightarrow \Lambda_c^{(*)} \ell^- \nu_\ell$  semi-leptonic decays with  $\ell^- = e^-$  (red solid line),  $\mu^-$  (blue dashed line),  $\tau^-$  (purple dot dashed line) and for  $\Lambda_c \rightarrow \Lambda^{(*)} \ell^+ \nu_\ell$  semi-leptonic decays with  $\ell^+ = e^+$  (red solid line),  $\mu^+$  (blue dashed line).

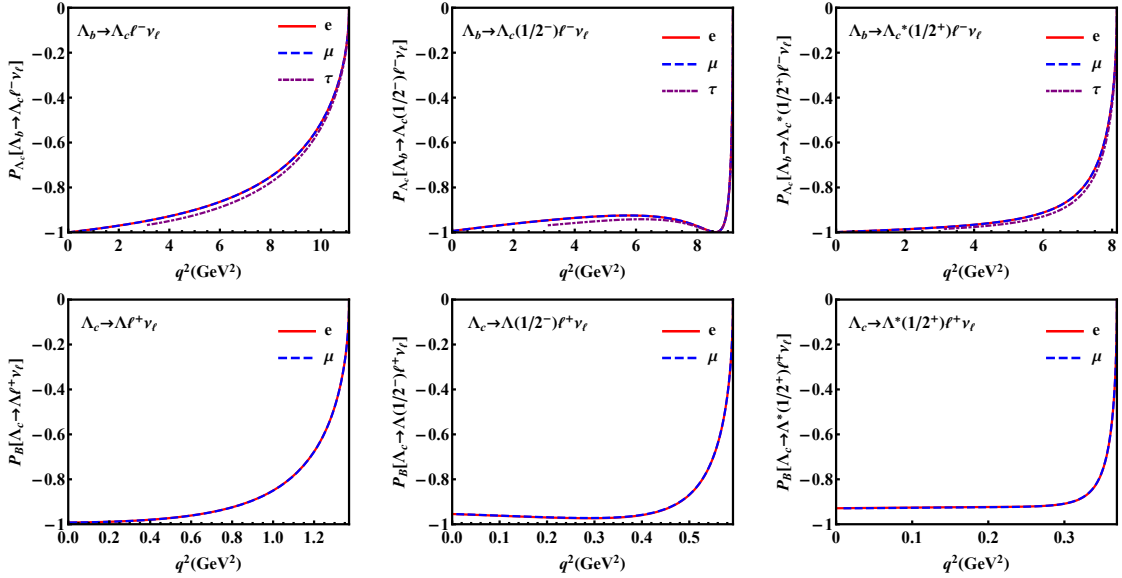


FIG. 5: The  $q^2$  dependence of final hadron longitudinal polarization ( $P_B$ ) for  $\Lambda_b \rightarrow \Lambda_c^{(*)} \ell^- \nu_\ell$  semi-leptonic decays with  $\ell^- = e^-$  (red solid line),  $\mu^-$  (blue dashed line),  $\tau^-$  (purple dot dashed line) and for  $\Lambda_c \rightarrow \Lambda^{(*)} \ell^+ \nu_\ell$  semi-leptonic decays with  $\ell^+ = e^+$  (red solid line),  $\mu^+$  (blue dashed line).

is consistent with [65]. The dependence on the lepton mass in the hadron polarization is less than the other physical observables. Our estimation of  $\langle P_B \rangle_{\Lambda_c \rightarrow \Lambda e^+ \nu_e} = -0.87$  agrees with  $-0.86 \pm 0.03 \pm 0.02$  [95] reported by CLEO Collaboration. In Fig. 6, the lepton polarization is close to  $P_\ell = -1$ , especially for electron modes. It stems from the weak interaction which is purely left-handed. With the negligible mass, the electron are approximately absolutely polarized. The line shapes of  $\mu$  and  $\tau$  modes can be understood by their masses

which change the chirality. As the  $q^2$  increases, the leptons are highly boosted, so that their helicity are more left-handed, with the polarization approaching to  $-1$ . The future experiments on the values of these observables and their comparison with the predictions of the present study would help us understand the corresponding channels and the internal structures of the baryons. Besides these observables are also important to investigate the new physics effects beyond the SM [114].

As the final talk, we would like to focus on the ratios of

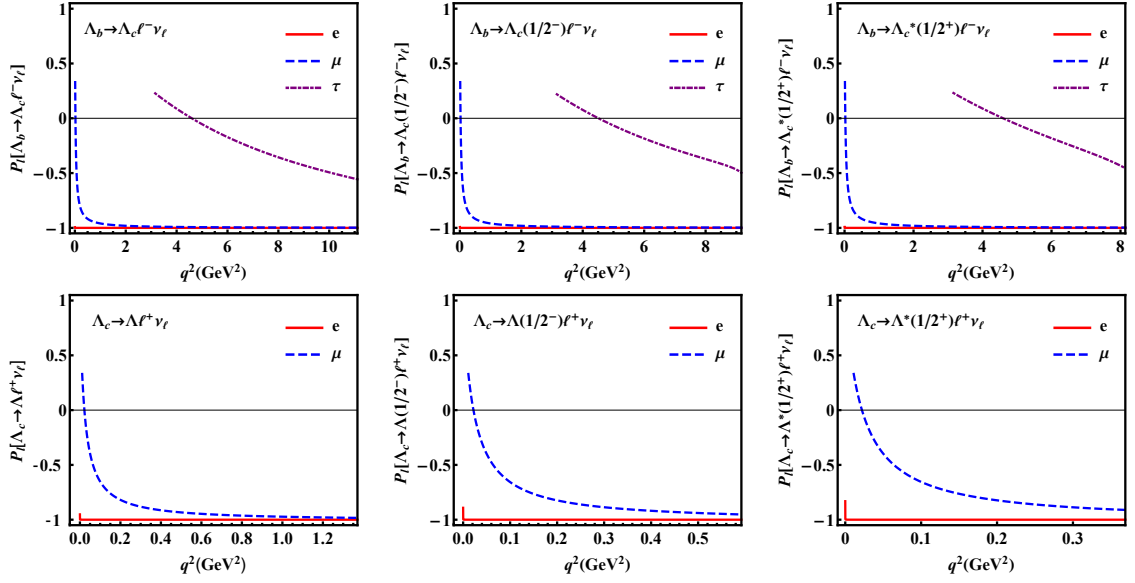


FIG. 6: The  $q^2$  dependence of final lepton longitudinal polarization ( $P_l$ ) for  $\Lambda_b \rightarrow \Lambda_c^{(*)} \ell^- \nu_\ell$  semi-leptonic decays with  $\ell^- = e^-$  (red solid line),  $\mu^-$  (blue dashed line),  $\tau^-$  (purple dot dashed line) and for  $\Lambda_c \rightarrow \Lambda^{(*)} \ell^+ \nu_\ell$  semi-leptonic decays with  $\ell^+ = e^+$  (red solid line),  $\mu^+$  (blue dashed line).

TABLE VIII: The predictions for averaged leptonic forward-backward asymmetry  $\langle A_{FB} \rangle$ , the averaged final hadron polarization  $\langle P_B \rangle$  and the averaged lepton polarization  $\langle P_\ell \rangle$ . The values in the same column for  $\Lambda_b \rightarrow \Lambda_c^{(*)} \ell^- \nu_\ell$  processes are the results for  $\ell^- = e^-, \mu^-, \tau^-$  up to down, while the ones for  $\Lambda_c \rightarrow \Lambda^{(*)} \ell^+ \nu_\ell$  processes are the results for  $\ell^+ = e^+, \mu^+$  up to down.

Channels	$\ell =$	$\langle A_{FB} \rangle$	$\langle P_B \rangle$	$\langle P_\ell \rangle$
$\Lambda_b \rightarrow \Lambda_c(1/2^+) \ell^- \nu_\ell$	$e$	0.18	-0.81	-1.00
	$\mu$	0.17	-0.81	-0.98
	$\tau$	-0.08	-0.77	-0.24
$\Lambda_b \rightarrow \Lambda_c(1/2^-) \ell^- \nu_\ell$	$e$	0.23	-0.95	-1.00
	$\mu$	0.22	-0.95	-0.98
	$\tau$	-0.07	-0.95	-0.18
$\Lambda_b \rightarrow \Lambda_c^*(1/2^+) \ell^- \nu_\ell$	$e$	0.18	-0.91	-1.00
	$\mu$	0.17	-0.91	-0.97
	$\tau$	-0.13	-0.88	-0.13
$\Lambda_c \rightarrow \Lambda(1/2^+) \ell^+ \nu_\ell$	$e$	0.20	-0.87	-1.00
	$\mu$	0.16	-0.87	-0.89
$\Lambda_c \rightarrow \Lambda(1/2^-) \ell^+ \nu_\ell$	$e$	0.18	-0.91	-1.00
	$\mu$	0.10	-0.91	-0.80
$\Lambda_c \rightarrow \Lambda^*(1/2^+) \ell^+ \nu_\ell$	$e$	0.11	-0.90	-1.00
	$\mu$	-0.001	-0.90	-0.71

branching fractions which reflect the leptonic flavour universality

$$R(\Lambda_c^{(*)}) = \frac{Br(\Lambda_b \rightarrow \Lambda_c^{(*)} \tau^- \nu_\tau)}{Br(\Lambda_b \rightarrow \Lambda_c^{(*)} \ell^- \nu_\ell)}, \quad (42)$$

with  $\ell^- = e^-$  or  $\mu^-$ . These ratios, obtained by our and other approaches, e.g. QCDSR [62], various quark models [38, 53, 56, 97], the SU(3) flavor symmetry [115], as well as LQCD [11, 116], are displayed in Table IX. Our estimation for  $R(\Lambda_c)$

TABLE IX: Our predictions for the ratios of branching fractions  $R(\Lambda_c^{(*)})$ .

	This work	Others
$R(\Lambda_c)$	0.32	about 0.3 [11, 53, 56, 62, 116]
$R(\Lambda_c(1/2^-))$	0.14	0.13 [56], 0.21-0.31 [38]
$R(\Lambda_c^*(1/2^+))$	0.06	

is consistent with other models. The  $\tau$ -channel for  $\Lambda_b \rightarrow \Lambda_c^*$  decays is smaller than the  $\Lambda_b \rightarrow \Lambda_c$  process, due to the smaller phase spaces.

## V. CONCLUSION AND DISCUSSION

In this work, we study the weak transition form factors for  $\Lambda_b \rightarrow \Lambda_c^{(*)}(1/2^\pm)$  and  $\Lambda_c \rightarrow \Lambda^{(*)}(1/2^\pm)$  in the framework of light-front quark model, and investigate the involved semi-leptonic decays. A semirelativistic three-body potential model and GEM are used to extract the baryon wave functions, which are as input of our calculation. This treatment of baryon wave functions is different from former way of taking a simple harmonic oscillator wave function with  $\beta$  value in the calculation. To some extent, we can avoid the  $\beta$  parameter dependence of result based on the support from baryon spectroscopy.

Our results of form factors for the ground-state modes are comparable to other theoretical studies, especially to the LQCD or HQL. The ones for the excited states involved modes need to be tested by more theories. These form factors will be useful for studying the weak decays of  $\Lambda_b$  and  $\Lambda_c$ .

With the obtained form factors, we predict the branching



fractions of the considered channels. Our results are consistent with the experimental data or the LQCD calculations. Especially, the excited-state modes have much smaller branching fractions compared to the ground-state modes, which can explain the measured result of  $\mathcal{B}(\Lambda_c \rightarrow \Lambda e^+ \nu_e)/\mathcal{B}(\Lambda_c \rightarrow e^+ X) = (91.9 \pm 13.6)\%$ . The ratios of  $R(\Lambda_c^{(*)}) = \mathcal{B}(\Lambda_b \rightarrow \Lambda_c^{(*)} \tau^- \nu_\tau)/\mathcal{B}(\Lambda_b \rightarrow \Lambda_c^{(*)} \ell^- \nu_\ell)$  are predicted to be tested for the lepton flavor universality. Moreover, the leptonic forward-backward asymmetry ( $A_{FB}$ ), the final hadron polarization ( $P_B$ ) and the lepton polarization ( $P_\ell$ ) are also investigated. The future BESIII, LHCb and Belle II experiments can measure these observables and test our results.

## ACKNOWLEDGMENTS

We would like to thank Chun-Khiang Chua, Si-Qiang Luo and Jian-Peng Wang for useful discussions. This work is supported by the China National Funds for Distinguished Young Scientists under Grant No. 11825503, National Key Research and Development Program of China under Contract No. 2020YFA0406400, the 111 Project under Grant No. B20063, and the National Natural Science Foundation of China under Grant No. 11975112 and 12047501.

- 
- [1] R. Aaij *et al.* [LHCb], Observation of the doubly charmed baryon  $\Xi_{cc}^{++}$ , Phys. Rev. Lett. **119** (2017) no.11, 112001.
- [2] R. Aaij *et al.* [LHCb], First Observation of the Doubly Charmed Baryon Decay  $\Xi_{cc}^{++} \rightarrow \Xi_c^+ \pi^+$ , Phys. Rev. Lett. **121** (2018) no.16, 162002.
- [3] A. Zupanc *et al.* [Belle], Measurement of the Branching Fraction  $\mathcal{B}(\Lambda_c^+ \rightarrow p K^+ \pi^+)$ , Phys. Rev. Lett. **113** (2014) no.4, 042002.
- [4] M. Ablikim *et al.* [BESIII], Measurement of the absolute branching fraction for  $\Lambda_c^+ \rightarrow \Lambda e^+ \nu_e$ , Phys. Rev. Lett. **115** (2015) no.22, 221805.
- [5] M. Ablikim *et al.* [BESIII], Measurements of absolute hadronic branching fractions of  $\Lambda_c^+$  baryon, Phys. Rev. Lett. **116** (2016) no.5, 052001.
- [6] M. Ablikim *et al.* [BESIII], Measurement of the absolute branching fraction for  $\Lambda_c^+ \rightarrow \Lambda \mu^+ \nu_\mu$ , Phys. Lett. B **767** (2017), 42-47.
- [7] M. Ablikim *et al.* [BESIII], Measurement of the absolute branching fraction of the inclusive semileptonic  $\Lambda_c^+$  decay, Phys. Rev. Lett. **121** (2018) no.25, 251801.
- [8] Y. B. Li *et al.* [Belle], First Measurements of Absolute Branching Fractions of the  $\Xi_c^0$  Baryon at Belle, Phys. Rev. Lett. **122** (2019) no.8, 082001.
- [9] R. Aaij *et al.* [LHCb], Measurement of matter-antimatter differences in beauty baryon decays, Nature Phys. **13** (2017), 391-396.
- [10] Y. S. Amhis *et al.* [HFLAV], Averages of  $b$ -hadron,  $c$ -hadron, and  $\tau$ -lepton properties as of 2018.
- [11] F. U. Bernlochner, Z. Ligeti, D. J. Robinson and W. L. Sutcliffe, Precise predictions for  $\Lambda_b \rightarrow \Lambda_c$  semileptonic decays, Phys. Rev. D **99** (2019) no.5, 055008.
- [12] F. U. Bernlochner, Z. Ligeti, D. J. Robinson and W. L. Sutcliffe, New predictions for  $\Lambda_b \rightarrow \Lambda_c$  semileptonic decays and tests of heavy quark symmetry, Phys. Rev. Lett. **121** (2018) no.20, 202001.
- [13] F. U. Bernlochner, M. F. Sevilla, D. J. Robinson and G. Wormser, Semitaonic  $b$ -hadron decays: A lepton flavor universality laboratory, [arXiv:2101.08326 [hep-ex]].
- [14] P. A. Zyla *et al.* [Particle Data Group], Review of Particle Physics, PTEP **2020** (2020) no.8, 083C01.
- [15] F. S. Yu, H. Y. Jiang, R. H. Li, C. D. Lü, W. Wang and Z. X. Zhao, Discovery Potentials of Doubly Charmed Baryons, Chin. Phys. C **42** (2018) no.5, 051001.
- [16] W. Wang, F. S. Yu and Z. X. Zhao, Weak decays of doubly heavy baryons: the  $1/2 \rightarrow 1/2$  case, Eur. Phys. J. C **77** (2017) no.11, 781.
- [17] J. J. Han, H. Y. Jiang, W. Liu, Z. J. Xiao and F. S. Yu, Rescattering mechanism of weak decays of double-charm baryons, [arXiv:2101.12019 [hep-ph]].
- [18] F. S. Yu, Role of decay in the search for double-charm baryons, Sci. China Phys. Mech. Astron. **63** (2020) no.2, 221065.
- [19] C. K. Chua, Color-allowed bottom baryon to  $s$ -wave and  $p$ -wave charmed baryon nonleptonic decays, Phys. Rev. D **100** (2019) no.3, 034025.
- [20] J. Zhu, Z. T. Wei and H. W. Ke, Semileptonic and nonleptonic weak decays of  $\Lambda_b^0$ , Phys. Rev. D **99** (2019) no.5, 054020.
- [21] H. W. Ke, X. Q. Li and Z. T. Wei, Diquarks and  $\Lambda_b \rightarrow \Lambda_c$  weak decays, Phys. Rev. D **77** (2008), 014020.
- [22] C. K. Chua, Color-allowed bottom baryon to charmed baryon nonleptonic decays, Phys. Rev. D **99** (2019) no.1, 014023.
- [23] Z. X. Zhao, Weak decays of heavy baryons in the light-front approach, Chin. Phys. C **42** (2018) no.9, 093101.
- [24] H. W. Ke, N. Hao and X. Q. Li, Revisiting  $\Lambda_b \rightarrow \Lambda_c$  and  $\Sigma_b \rightarrow \Sigma_c$  weak decays in the light-front quark model, Eur. Phys. J. C **79** (2019) no.6, 540.
- [25] C. Q. Geng, C. C. Lih, C. W. Liu and T. H. Tsai, Semileptonic decays of  $\Lambda_c^+$  in dynamical approaches, Phys. Rev. D **101** (2020) no.9, 094017.
- [26] H. C. Ballagh, H. H. Bingham, T. Lawry, G. R. Lynch, J. Lys, J. Orthel, M. D. Sokoloff, M. L. Stevenson, G. P. Yost and D. Gee, *et al.* Dilepton Production by Neutrinos in the Fermilab 15-ft Bubble Chamber, Phys. Rev. D **24** (1981), 7.
- [27] E. Vella, G. Trilling, G. S. Abrams, M. S. Alam, C. A. Blocker, A. Blondel, A. Boyarski, M. Breidenbach, D. L. Burke and W. C. Carithers, *et al.* Observation of Semileptonic Decays of Charmed Baryons, Phys. Rev. Lett. **48** (1982), 1515.
- [28] S. Klein, T. Himel, G. S. Abrams, D. Amidei, A. R. Baden, T. Barklow, A. Boyarski, J. Boyer, P. Burchat and D. L. Burke, *et al.*  $\Lambda_c^+$  Production and Semileptonic Decay in 29-GeV  $e^+ e^-$  Annihilation, Phys. Rev. Lett. **62** (1989), 2444.
- [29] H. Albrecht *et al.* [ARGUS], Observations of  $\Lambda_c^+$  semileptonic decay, Phys. Lett. B **269** (1991), 234-242.
- [30] T. Bergfeld *et al.* [CLEO], Study of the decay  $\Lambda_c^+ \rightarrow \Lambda e^+ \nu_\ell$ , Phys. Lett. B **323** (1994), 219-226.
- [31] R. Perez-Marcial, R. Huerta, A. Garcia and M. Avila-Aoki, Predictions for Semileptonic Decays of Charm Baryons. 2. Nonrelativistic and MIT Bag Quark Models, Phys. Rev. D **40** (1989), 2955 [erratum: Phys. Rev. D **44** (1991), 2203].
- [32] F. Hussain and J. G. Korner, Semileptonic charm baryon decays in the relativistic spectator quark model, Z. Phys. C **51** (1991), 607-614.

- [33] G. V. Efimov, M. A. Ivanov and V. E. Lyubovitskij, Predictions for semileptonic decay rates of charmed baryons in the quark confinement model, *Z. Phys. C* **52** (1991), 149-158.
- [34] H. Y. Cheng and B. Tseng,  $1/M$  corrections to baryonic form-factors in the quark model, *Phys. Rev. D* **53** (1996), 1457 [erratum: *Phys. Rev. D* **55** (1997), 1697].
- [35] R. S. Marques de Carvalho, F. S. Navarra, M. Nielsen, E. Ferreira and H. G. Dosch, Form-factors and decay rates for heavy Lambda semileptonic decays from QCD sum rules, *Phys. Rev. D* **60** (1999), 034009.
- [36] Y. L. Liu, M. Q. Huang and D. W. Wang, Improved analysis on the semi-leptonic decay  $\Lambda_c \rightarrow \Lambda \ell^+ \nu$  from QCD light-cone sum rules, *Phys. Rev. D* **80** (2009), 074011.
- [37] Z. X. Zhao, R. H. Li, Y. L. Shen, Y. J. Shi and Y. S. Yang, The semi-leptonic form factors of  $\Lambda_b \rightarrow \Lambda_c$  and  $\Xi_b \rightarrow \Xi_c$  in QCD sum rules, *Eur. Phys. J. C* **80** (2020) no.12, 1181.
- [38] M. Pervin, W. Roberts and S. Capstick, Semileptonic decays of heavy lambda baryons in a quark model, *Phys. Rev. C* **72** (2005), 035201.
- [39] S. Migura, D. Merten, B. Metsch and H. R. Petry, Semileptonic decays of baryons in a relativistic quark model, *Eur. Phys. J. A* **28** (2006), 55.
- [40] R. N. Faustov and V. O. Galkin, Semileptonic Decays of Heavy Baryons in the Relativistic Quark Model, *Particles* **3** (2020) no.1, 208-222.
- [41] T. Gutsche, M. A. Ivanov, J. G. Korner, V. E. Lyubovitskij and P. Santorelli, Semileptonic decays  $\Lambda_c^+ \rightarrow \Lambda \ell^+ \nu_\ell$  ( $\ell = e, \mu$ ) in the covariant quark model and comparison with the new absolute branching fraction measurements of Belle and BESIII, *Phys. Rev. D* **93** (2016) no.3, 034008.
- [42] R. L. Singleton, Semileptonic baryon decays with a heavy quark, *Phys. Rev. D* **43** (1991), 2939-2950.
- [43] T. Mannel, W. Roberts and Z. Ryzak,  $1/m_c$  suppressed semileptonic  $\Lambda_b$  decays, *Phys. Lett. B* **271** (1991), 421-424.
- [44] J. G. Korner and M. Kramer, Polarization effects in exclusive semileptonic  $\Lambda_c$  and  $\Lambda_b$  charm and bottom baryon decays, *Phys. Lett. B* **275** (1992), 495-505.
- [45] T. Mannel and G. A. Schuler, Semileptonic decays of bottom baryons at LEP, *Phys. Lett. B* **279** (1992), 194-200.
- [46] Y. B. Dai, C. S. Huang, M. Q. Huang and C. Liu, QCD sum rule analysis for the  $\Lambda_b \rightarrow \Lambda_c$  semileptonic decay, *Phys. Lett. B* **387** (1996), 379-385.
- [47] J. P. Lee, C. Liu and H. S. Song, Analysis of  $\Lambda_b \rightarrow \Lambda_c$  weak decays in heavy quark effective theory, *Phys. Rev. D* **58** (1998), 014013.
- [48] M. A. Ivanov, J. G. Korner, V. E. Lyubovitskij and A. G. Rusetsky, Charm and bottom baryon decays in the Bethe-Salpeter approach: Heavy to heavy semileptonic transitions, *Phys. Rev. D* **59** (1999), 074016.
- [49] F. Cardarelli and S. Simula, Analysis of the  $\Lambda_b \rightarrow \Lambda_c^+ \ell \bar{\nu}_\ell$  decay within a light front constituent quark model, *Phys. Rev. D* **60** (1999), 074018.
- [50] X. H. Guo, A. W. Thomas and A. G. Williams,  $1/m_Q$  corrections to the Bethe-Salpeter equation for  $\Lambda_Q$  in the diquark picture, *Phys. Rev. D* **61** (2000), 116015.
- [51] J. P. Lees *et al.* [BaBar], Evidence for an excess of  $\bar{B} \rightarrow D^{(*)} \tau^- \bar{\nu}_\tau$  decays, *Phys. Rev. Lett.* **109** (2012), 101802.
- [52] G. Caria *et al.* [Belle], Measurement of  $\mathcal{R}(D)$  and  $\mathcal{R}(D^*)$  with a semileptonic tagging method, *Phys. Rev. Lett.* **124** (2020) no.16, 161803.
- [53] R. N. Faustov and V. O. Galkin, Semileptonic decays of  $\Lambda_b$  baryons in the relativistic quark model, *Phys. Rev. D* **94** (2016) no.7, 073008.
- [54] D. Ebert, R. N. Faustov and V. O. Galkin, Semileptonic decays of heavy baryons in the relativistic quark model, *Phys. Rev. D* **73** (2006), 094002.
- [55] T. Gutsche, M. A. Ivanov, J. G. Körner, V. E. Lyubovitskij, P. Santorelli and N. Haby, Semileptonic decay  $\Lambda_b \rightarrow \Lambda_c + \tau^- + \bar{\nu}_\tau$  in the covariant confined quark model, *Phys. Rev. D* **91** (2015) no.7, 074001 [erratum: *Phys. Rev. D* **91** (2015) no.11, 119907].
- [56] T. Gutsche, M. A. Ivanov, J. G. Körner, V. E. Lyubovitskij, P. Santorelli and C. T. Tran, Analyzing lepton flavor universality in the decays  $\Lambda_b \rightarrow \Lambda_c^{(*)}(\frac{1}{2}^\pm, \frac{3}{2}^\pm) + \ell \bar{\nu}_\ell$ , *Phys. Rev. D* **98** (2018) no.5, 053003.
- [57] S. Rahmani, H. Hassanabadi and J. Kříž, Nonleptonic and semileptonic  $\Lambda_b \rightarrow \Lambda_c$  transitions in a potential quark model, *Eur. Phys. J. C* **80** (2020) no.7, 636.
- [58] K. Thakkar, Semileptonic transition of  $\Lambda_b$  baryon, *Eur. Phys. J. C* **80** (2020) no.10, 926.
- [59] D. W. Wang and M. Q. Huang, Choice of heavy baryon currents in QCD sum rules, *Phys. Rev. D* **67** (2003), 074025.
- [60] M. Q. Huang, H. Y. Jin, J. G. Korner and C. Liu, Note on the slope parameter of the baryonic  $\Lambda_b \rightarrow \Lambda_c$  Isgur-Wise function, *Phys. Lett. B* **629** (2005), 27-32.
- [61] Z. G. Wang, Analysis of the Isgur-Wise function of the  $\Lambda_b \rightarrow \Lambda_c$  transition with light-cone QCD sum rules, [arXiv:0906.4206 [hep-ph]].
- [62] K. Azizi and J. Y. Süngü, Semileptonic  $\Lambda_b \rightarrow \Lambda_c \ell \bar{\nu}_\ell$  Transition in Full QCD, *Phys. Rev. D* **97** (2018) no.7, 074007.
- [63] M. M. Hussain and W. Roberts,  $\Lambda_c$  Semileptonic Decays in a Quark Model, *Phys. Rev. D* **95** (2017) no.5, 053005.
- [64] J. Nieves, R. Pavao and S. Sakai,  $\Lambda_b$  decays into  $\Lambda_c^* \ell \bar{\nu}_\ell$  and  $\Lambda_c^* \pi^-$  [ $\Lambda_c^* = \Lambda_c(2595)$  and  $\Lambda_c(2625)$ ] and heavy quark spin symmetry, *Eur. Phys. J. C* **79** (2019) no.5, 417.
- [65] D. Bečirević, A. Le Yaouanc, V. Morénas and L. Oliver, Heavy baryon wave functions, Bakamjian-Thomas approach to form factors, and observables in  $\Lambda_b \rightarrow \Lambda_c(\frac{1}{2}^\pm) \ell \bar{\nu}$  transitions, *Phys. Rev. D* **102** (2020) no.9, 094023.
- [66] M. Ablikim *et al.* [BESIII], Future Physics Programme of BESIII, *Chin. Phys. C* **44** (2020) no.4, 040001.
- [67] K. C. Bowler *et al.* [UKQCD], First lattice study of semileptonic decays of  $\Lambda_b$  and  $\Xi_b$  baryons, *Phys. Rev. D* **57** (1998), 6948-6974.
- [68] S. A. Gottlieb and S. Tamhankar, A Lattice study of  $\Lambda_b$  semileptonic decay, *Nucl. Phys. B Proc. Suppl.* **119** (2003), 644-646.
- [69] S. Meinel,  $\Lambda_c \rightarrow \Lambda l^+ \nu_l$  form factors and decay rates from lattice QCD with physical quark masses, *Phys. Rev. Lett.* **118** (2017) no.8, 082001.
- [70] S. Meinel and G. Rendon,  $\Lambda_b \rightarrow \Lambda_c^*(2595, 2625) \ell^- \bar{\nu}$  form factors from lattice QCD, [arXiv:2103.08775 [hep-lat]].
- [71] W. Detmold, C. Lehner and S. Meinel,  $\Lambda_b \rightarrow p \ell^- \bar{\nu}_\ell$  and  $\Lambda_b \rightarrow \Lambda_c \ell^- \bar{\nu}_\ell$  form factors from lattice QCD with relativistic heavy quarks, *Phys. Rev. D* **92** (2015) no.3, 034503.
- [72] H. Y. Cheng, C. K. Chua and C. W. Hwang, Light front approach for heavy pentaquark transitions, *Phys. Rev. D* **70** (2004), 034007.
- [73] Z. T. Wei, H. W. Ke and X. Q. Li, Evaluating decay Rates and Asymmetries of  $\Lambda_b$  into Light Baryons in LFQM, *Phys. Rev. D* **80** (2009), 094016.
- [74] Q. Chang, L. T. Wang and X. N. Li, Form factors of  $V' \rightarrow V''$  transition within the light-front quark models, *JHEP* **12** (2019), 102.
- [75] Q. Chang, X. L. Wang and L. T. Wang, Tensor form factors of  $P \rightarrow P, S, V$  and  $A$  transitions within standard and covariant light-front approaches, *Chin. Phys. C* **44** (2020) no.8, 083105.

- [76] H. W. Ke, F. Lu, X. H. Liu and X. Q. Li, Study on  $\Xi_{cc} \rightarrow \Xi_c$  and  $\Xi_{cc} \rightarrow \Xi'_c$  weak decays in the light-front quark model, *Eur. Phys. J. C* **80** (2020) no.2, 140.
- [77] H. W. Ke, X. H. Yuan, X. Q. Li, Z. T. Wei and Y. X. Zhang,  $\Sigma_b \rightarrow \Sigma_c$  and  $\Omega_b \rightarrow \Omega_c$  weak decays in the light-front quark model, *Phys. Rev. D* **86** (2012), 114005.
- [78] S. Godfrey and N. Isgur, Mesons in a Relativized Quark Model with Chromodynamics, *Phys. Rev. D* **32** (1985), 189-231.
- [79] S. Capstick and N. Isgur, Baryons in a Relativized Quark Model with Chromodynamics, *AIP Conf. Proc.* **132** (1985), 267-271.
- [80] Q. T. Song, D. Y. Chen, X. Liu and T. Matsuki, Charmed-strange mesons revisited: mass spectra and strong decays, *Phys. Rev. D* **91** (2015), 054031.
- [81] C. Q. Pang, J. Z. Wang, X. Liu and T. Matsuki, A systematic study of mass spectra and strong decay of strange mesons, *Eur. Phys. J. C* **77** (2017) no.12, 861.
- [82] J. Z. Wang, Z. F. Sun, X. Liu and T. Matsuki, Higher bottomonium zoo, *Eur. Phys. J. C* **78** (2018) no.11, 915.
- [83] E. Hiyama, Y. Kino and M. Kamimura, Gaussian expansion method for few-body systems, *Prog. Part. Nucl. Phys.* **51** (2003), 223-307.
- [84] T. Yoshida, E. Hiyama, A. Hosaka, M. Oka and K. Sadato, Spectrum of heavy baryons in the quark model, *Phys. Rev. D* **92** (2015) no.11, 114029.
- [85] G. Yang, J. Ping, P. G. Ortega and J. Segovia, Triply heavy baryons in the constituent quark model, *Chin. Phys. C* **44** (2020) no.2, 023102.
- [86] J. M. M. Hall, W. Kamleh, D. B. Leinweber, B. J. Menadue, B. J. Owen, A. W. Thomas and R. D. Young, Lattice QCD Evidence that the  $\Lambda(1405)$  Resonance is an Antikaon-Nucleon Molecule, *Phys. Rev. Lett.* **114** (2015) no.13, 132002.
- [87] Z. W. Liu, J. M. M. Hall, D. B. Leinweber, A. W. Thomas and J. J. Wu, Structure of the  $\Lambda(1405)$  from Hamiltonian effective field theory, *Phys. Rev. D* **95** (2017) no.1, 014506.
- [88] K. Azizi, B. Barsbay and H. Sundu, Mass and residue of  $\Lambda(1405)$  as hybrid and excited ordinary baryon, *Eur. Phys. J. Plus* **133** (2018) no.3, 121.
- [89] M. Mai, Review of the  $\Lambda(1405)$ : A curious case of a strangeness resonance, [arXiv:2010.00056 [nucl-th]].
- [90] K. Chen, H. W. Ke, X. Liu and T. Matsuki, Estimating the production rates of  $D$ -wave charmed mesons via the semileptonic decays of bottom mesons, *Chin. Phys. C* **43** (2019) no.2, 023106.
- [91] H. Xu, Q. Huang, H. W. Ke and X. Liu, Numerical analysis of the production of  $D^{(*)}(3000)$ ,  $D_{sJ}(3040)$  and their partners through the semileptonic decays of  $B_{(s)}$  mesons in terms of the light front quark model, *Phys. Rev. D* **90** (2014) no.9, 094017.
- [92] H. Georgi, B. Grinstein and M. B. Wise,  $\Lambda_b$  semileptonic decay form-factors for  $m_c$  does not equal infinity, *Phys. Lett. B* **252** (1990), 456-460.
- [93] J. Abdallah *et al.* [DELPHI Collaboration], Measurement of the  $\Lambda_b^0$  decay form-factor, *Phys. Lett. B* **585**, 63 (2004).
- [94] R. Aaij *et al.* [LHCb Collaboration], Measurement of the shape of the  $\Lambda_b^0 \rightarrow \Lambda_c^+ \mu^- \bar{\nu}_\mu$  differential decay rate, *Phys. Rev. D* **96**, no. 11, 112005 (2017).
- [95] J. W. Hinson *et al.* [CLEO], Improved measurement of the form-factors in the decay  $\Lambda_c^+ \rightarrow \Lambda e^+ \nu_e$ , *Phys. Rev. Lett.* **94** (2005), 191801.
- [96] M. Q. Huang and D. W. Wang, semi-leptonic decay  $\Lambda_c \rightarrow \Lambda \ell^+ \nu$  from QCD light-cone sum rules, [arXiv:hep-ph/0608170 [hep-ph]].
- [97] R. N. Faustov and V. O. Galkin, semi-leptonic decays of  $\Lambda_c$  baryons in the relativistic quark model, *Eur. Phys. J. C* **76**, no. 11, 628 (2016).
- [98] C. D. Lü, W. Wang and F. S. Yu, *Test flavor SU(3) symmetry in exclusive  $\Lambda_c$  decays*, *Phys. Rev. D* **93**, no.5, 056008 (2016) [arXiv:1601.04241 [hep-ph]].
- [99] C. Q. Geng, Y. K. Hsiao, Y. H. Lin and L. L. Liu, *Non-leptonic two-body weak decays of  $\Lambda_c(2286)$* , *Phys. Lett. B* **776**, 265-269 (2018) [arXiv:1708.02460 [hep-ph]].
- [100] C. Q. Geng, Y. K. Hsiao, C. W. Liu and T. H. Tsai, *Charmed Baryon Weak Decays with SU(3) Flavor Symmetry*, *JHEP* **11**, 147 (2017) [arXiv:1709.00808 [hep-ph]].
- [101] D. Wang, P. F. Guo, W. H. Long and F. S. Yu,  $K_S^0 - K_L^0$  asymmetries and CP violation in charmed baryon decays into neutral kaons, *JHEP* **03**, 066 (2018) [arXiv:1709.09873 [hep-ph]].
- [102] C. Q. Geng, Y. K. Hsiao, C. W. Liu and T. H. Tsai, *Antitriplet charmed baryon decays with SU(3) flavor symmetry*, *Phys. Rev. D* **97**, no.7, 073006 (2018) [arXiv:1801.03276 [hep-ph]].
- [103] H. Y. Cheng, X. W. Kang and F. Xu, *Singly Cabibbo-suppressed hadronic decays of  $\Lambda_c^+$* , *Phys. Rev. D* **97**, no.7, 074028 (2018) [arXiv:1801.08625 [hep-ph]].
- [104] H. Y. Jiang and F. S. Yu, *Fragmentation-fraction ratio  $f_{\Xi_b}/f_{\Lambda_b}$  in  $b$ - and  $c$ -baryon decays*, *Eur. Phys. J. C* **78**, no.3, 224 (2018) [arXiv:1802.02948 [hep-ph]].
- [105] C. Q. Geng, Y. K. Hsiao, C. W. Liu and T. H. Tsai, *SU(3) symmetry breaking in charmed baryon decays*, *Eur. Phys. J. C* **78**, no.7, 593 (2018) [arXiv:1804.01666 [hep-ph]].
- [106] C. Q. Geng, Y. K. Hsiao, C. W. Liu and T. H. Tsai, *Three-body charmed baryon Decays with SU(3) flavor symmetry*, *Phys. Rev. D* **99**, no.7, 073003 (2019) [arXiv:1810.01079 [hep-ph]].
- [107] H. J. Zhao, Y. L. Wang, Y. K. Hsiao and Y. Yu, *A diagrammatic analysis of two-body charmed baryon decays with flavor symmetry*, *JHEP* **02**, 165 (2020) [arXiv:1811.07265 [hep-ph]].
- [108] C. P. Jia, D. Wang and F. S. Yu, *Charmed baryon decays in SU(3)<sub>F</sub> symmetry*, *Nucl. Phys. B* **956**, 115048 (2020) [arXiv:1910.00876 [hep-ph]].
- [109] J. Zou, F. Xu, G. Meng and H. Y. Cheng, *Two-body hadronic weak decays of antitriplet charmed baryons*, *Phys. Rev. D* **101**, no.1, 014011 (2020) [arXiv:1910.13626 [hep-ph]].
- [110] P. Y. Niu, J. M. Richard, Q. Wang and Q. Zhao, *Hadronic weak decays of  $\Lambda_c$  in the quark model*, *Phys. Rev. D* **102**, no.7, 073005 (2020) [arXiv:2003.09323 [hep-ph]].
- [111] G. Meng, S. M. Y. Wong and F. Xu, *Doubly Cabibbo-suppressed decays of antitriplet charmed baryons*, *JHEP* **11**, 126 (2020) [arXiv:2005.12111 [hep-ph]].
- [112] S. Hu, G. Meng and F. Xu, *Hadronic weak decays of the charmed baryon  $\Omega_c$* , *Phys. Rev. D* **101**, no.9, 094033 (2020) [arXiv:2003.04705 [hep-ph]].
- [113] R. Aaij *et al.* [LHCb], Precision measurement of the  $\Lambda_c^+$ ,  $\Xi_c^+$  and  $\Xi_c^0$  baryon lifetimes, *Phys. Rev. D* **100** (2019) no.3, 032001.
- [114] K. Azizi, A. T. Olgun and Z. Tavukoğlu, "Effects of vector leptoquarks on  $\Lambda_b \rightarrow \Lambda_c \ell \bar{\nu}_\ell$  decay," *Chin. Phys. C* **45** (2021) no.1, 013113.
- [115] C. Geng, C. Liu, T. Tsai and S. Yeh, semi-leptonic decays of anti-triplet charmed baryons, *Phys. Lett. B* **792** (2019), 214-218.
- [116] X. Mu, Y. Li, Z. Zou and B. Zhu, Investigation of effects of new physics in  $\Lambda_b \rightarrow \Lambda_c \tau \bar{\nu}_\tau$  decay, *Phys. Rev. D* **100** (2019) no.11, 113004.